

Spatially structured superinfection and the evolution of disease virulence

Thomas Caraco, Stephan Glavanakov,

Department of Biological Sciences, University at Albany, Albany, New York 12222

Shengua Li, William Maniatty,

Department of Computer Science, University at Albany, Albany, New York 12222

Boleslaw K. Szymanski

Department of Computer Science, Rensselaer Polytechnic Institute, Troy, New York 12180

Address for manuscript correspondence:

Thomas Caraco, Dept. Biological Sciences, University at Albany, Albany, NY 12222 USA

e-mail: caraco@albany.edu

phone: 518-442-4343

Abstract

When pathogen strains differing in virulence compete for hosts, spatial structuring of disease transmission can govern both evolved levels of virulence and patterns in strain coexistence. We develop a spatially detailed model of superinfection, a form of contest competition between pathogen strains; the probability of superinfection depends explicitly on the difference in levels of virulence. We apply methods of adaptive dynamics to address the interplay of spatial dynamics and evolution. The mean-field approximation predicts evolution to criticality; any small increase in virulence capable of dynamical persistence is favored. Both pair approximation and simulation of the detailed model indicate that spatial structure constrains disease virulence. Increased spatial clustering reduces the maximal virulence capable of single-strain persistence and, more importantly, reduces the convergent-stable virulence level under strain competition. The spatially detailed model predicts that increasing the probability of superinfection, for given difference in virulence, increases the likelihood of between-strain coexistence. When strains differing in virulence can coexist ecologically, our results may suggest policies for managing diseases with localized transmission. Comparing equilibrium densities from the pair approximation, we find that introducing a more virulent strain into a host population infected by a less virulent strain can sometimes reduce total host mortality and increase global host density.

Keywords: Adaptive dynamics, Spatial process, Superinfection, Virulence evolution

1. Introduction

When increased disease virulence accelerates transmission of infectious propagules between hosts, but simultaneously reduces the longevity of infection within hosts, changes in virulence can alter host-pathogen dynamics significantly (Bull, 1994; Ewald, 1994; Frank, 1996; Day, 2002; Holt and Hochberg, 2002). Population dynamics, in turn, sets the framework for the evolution of virulence (Castillo-Chavez and Velasco-Hernandez, 1998; van Baalen and Sabelis, 1995). In particular, spatially structured disease transmission can govern virulence evolution through effects on infection dynamics; locally structured infection generally favors virulence lower than predicted by homogeneous mixing of susceptible and infectious hosts (Haraguchi and Sasaki, 2000; van Baalen, 2002a). We present results on the evolution of virulence, defined here as the increase in host mortality due to disease. We model spatially structured superinfection, a form of contest competition between pathogen strains differing in virulence. To address the interaction of host-pathogen spatial processes and virulence evolution, we apply methods of adaptive dynamics (Geritz *et al.*, 1998; Pugliese, 2002a; Magori *et al.*, 2005).

Section 2 summarizes the hypothesis that pathogen-strain competition drives virulence evolution. Section 3 presents a spatially detailed model for pairwise strain competition; we assume asymmetric superinfection (Levin and Pimentel, 1981) where the chance of competitive displacement varies with the difference in virulence between strains. Section 4 summarizes a mean-field approximation to the spatial model, and Section 5 develops a pair approximation (Matsuda *et al.*, 1992; Hiebeler, 2000). Section 6 applies adaptive dynamics to both the pair approximation and simulations of the detailed model. The Discussion collects predictions, offers a simple perspective on virulence management, and comments on broader definitions of disease virulence (Antia *et al.*, 1994; O’Keefe and Antonovics, 2002; van Baalen, 2002b).

2. Pathogen-strain competition

Properties of transmission between hosts and resource exploitation within infected hosts define the mode of pathogen-strain competition. If infection of a host individual by one strain prevents infection of the same individual by a second strain (Bremermann and Thieme, 1989), competition is preemptive. Pathogen strains compete between hosts, and there is no within-host competition. If infectives and susceptibles mix homogeneously, preemptive strain competition may favor maximization of R_0 , a strain's basic reproduction number (expected number of new infections per infection in a population of susceptibles). Maximizing R_0 precludes coexistence; an optimally virulent strain reduces susceptible density so low that no other level of virulence can advance when rare (Bremermann and Thieme, 1989; van Baalen, 2002a).

Pathogen strains compete both between and within hosts under coinfection and superinfection. Coinfection assumes that different strains can infect, and concurrently be transmitted from, the same host individual (Bremermann and Pickering, 1983). van Baalen and Sabelis' (1995) assume that each of two strains exploiting the same host individual is transmitted less efficiently than when exploiting a host solitarily, so that coinfection resembles scramble competition. Superinfection implies contest competition. A more virulent strain can infect a host already infected by a less virulent strain, and then displace the less virulent strain (Levin and Pimentel, 1981; Castillo-Chavez and Velasco-Hernandez, 1998). Some models of the process permit two-way superinfection, but maintain a virulence-based competitive asymmetry (Gandon *et al.*, 2002; Pugliese, 2002a). Maniatty *et al.* (1998) generalize strain competition by decoupling superinfection from a virulence-based advantage in transmission rate.

Coinfection and superinfection may permit coexistence of pathogen strains under homogeneous mixing (Nowak and May, 1994; May and Nowak, 1995; Mosquera and Adler,

1998; see Saldaña *et al.*, 2003). For superinfection, Adler and Mosquera (2000) caution that multi-strain coexistence can result from assuming a discontinuous superinfection function, where a minimal increase in virulence implies a strong, deterministic advantage in contest competition. Smoothing the superinfection function, so that competitive advantage varies continuously with the difference in virulence levels, eliminates much of the multi-strain coexistence (Adler and Mosquera, 2000). Another consequence of discontinuous superinfection is that no resident strain will be evolutionarily stable, but for smoothed superinfection, Pugliese (2002a) finds conditions yielding a monomorphic, evolutionarily stable strategy (ESS) for virulence.

When selection acts on coinfecting or superinfecting pathogens, within-host competition diminishes an avirulent strain's benefit of an extended infectious period. A strain exploiting a host solitarily "anticipates" sharing host resources with a coinfecting strain, or losing the host entirely to a superinfecting strain. Either case can favor greater virulence, to exploit more host resources before a competitor arrives. A broad implication of these models is that different modes of strain competition generate different host-pathogen dynamics, and differences in the dynamics can have important effects on the evolution of virulence.

Spatial structuring of disease transmission can alter consequences of pathogen strain competition. If infectious contacts are spatially localized, disease ordinarily advances more slowly than under global mixing, and the difference depends on neighborhood size (Caraco *et al.*, 1998; Duryea *et al.*, 1999; Keeling, 1999; van Baalen, 2000). Local structuring of infection should then reduce evolved levels of virulence, compared to homogeneous mixing (Herre, 1993; van Baalen, 2002a). A more virulent strain infects nearby susceptibles faster, but the greater rate of host mortality generates spatial heterogeneity in the host population's density. Clusters of diseased hosts can become isolated from susceptibles, and the infection may fail to advance

(Sato *et al.*, 1994; Rand *et al.*, 1995). A less virulent strain, with an extended infectious period, might not outpace the local dynamics of its host, and so be able to advance globally.

Rand *et al.* (1995) and Haraguchi and Sasaki (2000), under different assumptions, demonstrate that spatially structured infection can favor reduced virulence (or lower transmission) when strains compete preemptively. Claessen and de Roos (1995) simulate coinfection with transmission limited to nearest neighbors, and find that evolutionarily stable virulence with global mixing may fail to predict results of a spatial model. Our study complements these analyses. We analyze disease virulence for spatially structured superinfection by applying adaptive dynamics (Kisdi and Meszéna, 1993; Geritz *et al.*, 1998; Pugliese, 2002a) to our model and its deterministic approximations.

3. Spatially detailed model of superinfection

Each dynamically equivalent site on a rectangular lattice, with J total sites, can be occupied by at most one host individual. Any site's local state belongs to the set $\{0, S, A, V\}$. We represent an empty site by 0. S identifies a site occupied by a susceptible host. A represents a site occupied by a host infected with a less virulent pathogen strain; for convenience we term this avirulent infection. V represents a site with a host infected by a more virulent pathogen, termed virulent infection.

Time t advances discretely, and we order events as follows. Reproduction is independent of infection status; offspring produced at time t join the host population as susceptibles at $(t + 1)$. Pathogens attack available hosts while the latter reproduce; new infections appear at $(t + 1)$. Next, all hosts alive at time t are subject to mortality; a host's survival depends on its infection status at the beginning of the period. At time $(t + 1)$ combined effects of birth, infection of susceptibles, superinfection, and mortality are realized. Infected hosts do not recover.

3.1. Parameters of the spatial model

Contact structure governs details of epidemiological invasion (Keeling, 1999; Korniss and Caraco, 2005). We assume nearest-neighbor interaction in both host dispersal and infection transmission. Hence an empty site may be colonized only by propagules dispersed from surrounding sites. $\sigma_c(k)$ represents the colonization neighborhood about site k ($k = 1, 2, \dots, J$). The number of sites in the neighborhood is $|\sigma_c(k)| = N$. If site k is empty, each host on $\sigma_c(k)$ independently places an offspring at the open site with probability b , the birth probability. Host reproductive effort remains constant as the size of the colonization neighborhood varies, so the per-site birth probability b declines with N . Let $b = B/N < 1$, where B represents a host's reproductive expenditure.

$\sigma_p(k)$ represents the infection neighborhood about site k ; infectious contacts are spatially structured. For simplicity, let $\sigma_p(k) = \sigma_c(k)$, so that colonization and infection neighborhoods become the same set of N nearest neighbors. If a susceptible occupies site k , each avirulently infected host on $\sigma_p(k)$ independently transmits that strain to site k with probability β_A . β_V is the virulent infection probability. If a susceptible or avirulently infected host occupies site k , each host on $\sigma_p(k)$ infected by the virulent strain independently transmits that pathogen strain to the site k with probability β_V . The total infectious propagules emanating from a host remains constant as the size of the transmission neighborhood varies, so $\beta_i \sim N^{-1}$; $i = A, V$. Since the host and pathogens disperse on the same neighborhood, we have $\sigma_c(k) = \sigma_p(k) = \sigma_k$.

Discrete-time dynamics allows both strains to be transmitted to the same susceptible during a single time interval. Transmission of the virulent strain to an avirulently infected host produces a similar situation. Each of these events generates contest competition, which is resolved via γ , the superinfection probability. If both strains attack the same susceptible, or

when the virulent strain attempts to superinfect an avirulently infected host, γ is the probability that the host, should it survive, develops a virulent infection. The virulent strain has an advantage in contest competition, so $\gamma \geq 1/2$; see section 3.2.

Following host and pathogen dispersal, each host independently dies or survives to the next time interval. Mortality probabilities depend on infection status. μ_S is the probability that a susceptible, alive at t , is dead at time $(t + 1)$. The mortality probability for an avirulently infected host is μ_A , and μ_V is the mortality probability for a virulently infected host. Given our definition of virulence, $\mu_S < \mu_A < \mu_V$.

Figure 1 diagrams feasible transitions for a single site. Table 1 lists symbols for the spatially detailed model. In Appendix A we derive expressions for the detailed model's transition probabilities.

3.2. Functional dependence of transmission and virulence

Details of transmission-virulence interactions remain unknown (Bryant and Behm, 1989; Antia *et al.*, 1994; Powell *et al.*, 2000; Ganusov and Antia, 2003). We consider two possibilities. First, suppose that β_i increases in a strictly monotonic, concave manner as μ_i increases:

$$\beta_i(\mu_i) = \mu_i^\alpha / N; \quad 0 < \alpha < 1; \quad i = A, V. \quad (1A)$$

The virulent strain has the greater per-infection probability of infecting a susceptible neighbor, but imposes an increased host-mortality probability. β_i/μ_i , the ratio of transmission to virulence, is the product of the transmission probability (per unit time) and the expected duration of the infection-transmission period. Since $0 < \alpha < 1$, the transmission to virulence ratio declines as virulence increases. Therefore, any greater capacity for interference competition (superinfection) implies a reduced capacity for “colonization” of susceptible hosts.

Secondly, we can suppose that the transmission probability reaches a maximum at intermediate virulence:

$$\beta_i(\mu_i) = f \frac{\mu_i^\alpha (1 - \mu_i)}{N}; \alpha > 0, f > 0; i = A, V. \quad (1B)$$

At low virulence levels, the infection-transmission probability increases with virulence, and then declines at sufficiently high virulence. The transmission to virulence ratio β_i/μ_i also can reach a maximum at intermediate virulence, implying that the best colonizers no longer are the least virulent strains (Nowak and May, 1994; Claessen and de Roos, 1995; Pugliese, 2002b). The constant f in Eq. (1B) lets us equate $\int (\beta_i/\mu_i) d\mu_i$ for the two transmission functions, simplifying comparisons of our computational results; note that we relax the constraint on the value of α in Eq (1B). Figure 2 shows the two transmission-probability functions of virulence, plotted with parameter values we use in analyses reported below.

The superinfection process is discontinuous in that only the virulent strain can exclude its competitor. But for any $\mu_V > \mu_A$, the superinfection probability γ depends continuously on the difference in host mortality probabilities, according to:

$$\gamma(\mu_V, \mu_A) = \left[1 + (\mu_V - \mu_A)^\psi \right] / 2; \psi > 0. \quad (2)$$

If $\psi < 1$, a small difference in virulence gives the virulent strain a strong competitive advantage through superinfection. If $\psi > 1$, a larger difference in virulence is required for the same competitive advantage; as ψ grows large, $\gamma \rightarrow 1/2$.

4. Mean-field approximation

We relegate details of the mean-field analysis to Appendix B and present the results here. Table 2 lists symbols introduced in this section.

$\rho_i(t)$ represents the global density of sites in state i at time t ; as above, $i \in \{0, S, A, V\}$.

For brevity, we restrict the mean-field analysis to disease-transmission probabilities that increase strictly monotonically with virulence, Eq. (1A). Mean-field approximation leads to a mass-action formulation for densities of susceptible, avirulently infected and virulently infected hosts:

$$\rho_S(t+1) = B (\rho_S + \rho_A + \rho_V) \rho_0 + \rho_S(t) [1 - \mu_A^\alpha \rho_A(t)] [1 - \mu_V^\alpha \rho_V(t)] (1 - \mu_S), \quad (3)$$

$$\rho_A(t+1) = \rho_A(t) [\mu_A^\alpha \rho_S(t) (1 - \mu_S) + (1 - \mu_A)] [1 - \gamma \mu_V^\alpha \rho_V(t)], \quad (4)$$

$$\rho_V(t+1) = \rho_V(t) \left\{ \begin{array}{l} \mu_V^\alpha \rho_S(t) (1 - \mu_S) [1 - (1 - \gamma) \mu_A^\alpha \rho_A(t)] \\ + \gamma \mu_V^\alpha \rho_A(t) (1 - \mu_A) + (1 - \mu_V) \end{array} \right\}. \quad (5)$$

The density of open sites, $\rho_0(t)$, follows from $\sum_i \rho_i(t) = 1$. We can express total host density as $\rho(t) = 1 - \rho_0(t)$.

In the absence of infection, the host population advances to a positive disease-free equilibrium where the global density of susceptibles is $\rho_S^* = 1 - \mu_S/B$, with $\mu_S < B$. Given a host population at the disease-free equilibrium, consider invasion by a single pathogen strain which induces a host-mortality probability $\mu_A > \mu_S$. Pathogen invasion requires that the strain's growth rate when rare exceed unity. Under homogeneous mixing this requirement reduces to:

$$\left(1 - \frac{\mu_S}{B}\right) (1 - \mu_S) > \mu_A^{1-\alpha}. \quad (6)$$

A high density of susceptibles promotes a single strain's initial advance, as does a large transmission to virulence ratio. That is, both low pathogen virulence (long infectious period), and high transmission of infection (α not too great) increase the rare pathogen's growth.

Assuming that the pathogen invades, infection advances to its single-strain endemic equilibrium, where the susceptible density becomes $\rho_S^* = \mu_A^{1-\alpha} / (1 - \mu_S)$. The corresponding density of infected hosts is:

$$\rho_A^* = \rho^* - \rho_S^* = \frac{B - \mu_A}{2B} + \frac{1}{2B} \left[(B - \mu_A)^2 + 4B\rho_S^* (\mu_A - \mu_S) \right]^{1/2} - \rho_S^*, \quad (7)$$

at the positive, single-strain equilibrium. Susceptible density declines, and the equilibrium density of infected hosts increases, as the transmission to virulence ratio increases. ρ_A^* increases as B increases, and declines as either μ_S or μ_A increases; greater virulence decreases the equilibrium density of infected hosts.

Given the single-strain endemic equilibrium, we turn to the mean-field's pairwise invasion criteria. Consider an avirulent and a virulent strain with (respective) host-mortality probabilities $\mu_A < \mu_V$. First, assume the avirulent strain is resident with density given by Eq. (7). The virulent strain invades if its increase when rare through infecting susceptibles and through superinfection exceeds losses through host mortality; invasion by the virulent strain requires:

$$\rho_A^* > (\mu_V^{1-\alpha} - \mu_A^{1-\alpha}) / (\gamma - \mu_A), \quad (8)$$

where the superinfection probability γ depends on the difference $(\mu_V - \mu_A)$.

Now assume the virulent strain is resident; global susceptible density is given by $\rho_S^* = \mu_V^{1-\alpha} / (1 - \mu_S)$, and infective density is given by Eq. (7) with μ_V replacing μ_A , and ρ_V replacing ρ_A . The avirulent strain invades if its increase when rare through transmission to susceptibles exceeds its losses through contest competition and host mortality; successful avirulent invasion requires:

$$\rho_V^* < \frac{\mu_A^\alpha \mu_V^{1-\alpha} - \mu_A}{\gamma \mu_V^\alpha (1 + \mu_A^\alpha \mu_V^{1-\alpha} - \mu_A)}. \quad (9)$$

If both (8) and (9) hold, the two strains can coexist ecologically. If ρ_A were great enough for (8) to hold, μ_A cannot be too large. If ρ_V were small enough for (9) to hold, μ_V cannot be too small. Virulence levels of the two strains must differ sufficiently for coexistence in the mean-field model. When the strains coexist, the avirulent type persists by finding enough susceptibles to infect, and the virulent strain maintains itself through interference competition.

To address virulence evolution in the mean-field model, suppose that mutants arise at the single-strain endemic equilibrium, and that host-mortality probabilities of the resident and mutant differ by a small amount ε . A virulent mutant invades a resident μ_A if expression (8) holds with $\mu_V = \mu_A + \varepsilon$. An avirulent mutant invades a resident μ_V if expression (9) holds with $\mu_A = \mu_V - \varepsilon$. As $\varepsilon \rightarrow 0$, the right-hand side of both (8) and (9) approaches 0. Hence, a virulent mutant invades successfully, but an avirulent mutant is repelled. Under the mean-field model, assuming mutations in virulence are small, virulence “evolves to criticality” (*cf.* Rand *et al.*, 1995). That is, virulence increases, as each more virulent mutant invades, until host mortality approaches $\left[\left(1 - \frac{\mu_s}{B} \right) (1 - \mu_s) \right]^{1/(1-\alpha)}$. Beyond this point, despite the increase in susceptible density with virulence, the rate of mortality among infected hosts becomes too great to sustain the pathogen (R_0 falls below unity; see Appendix B).

Figure 3 plots pairwise invasibility results for the mean-field model. If the difference in virulence between strains is small, the more virulent invader (resident) always invades and excludes (repels) the less virulent strain. Some strain combinations can coexist, if the difference in virulence is large enough. No monomorphic ESS is possible, and sequentially monomorphic populations (Geritz *et al.*, 1998) evolve to criticality. Note that R_0 declines and susceptible

density increases as virulence evolves, the outcome opposite that predicted for preemptive strain competition under homogeneous mixing (Bremermann and Thieme, 1989).

5. Pair approximation

Pair approximation models combinations of states at paired, neighboring sites (Matsuda *et al.*, 1992; Hiebeler, 2000). Dynamics of the pair-block frequencies reflects a degree of local spatial correlation, and consequently approximates most spatial processes better than mean-field models (Nakamura *et al.*, 1997; Ives *et al.*, 1998; Caraco *et al.*, 2001). Specifically, pair approximation assumes that the correlation between states of two neighboring does not depend on the state of any other, randomly selected neighbor of the focal pair. This assumption closes the pair approximation's system of equations, but ignores the more extensive spatial correlations that can affect the dynamics. For more extensive methods, see Rand (1999), Sato and Iwasa (2000) or van Baalen (2000). Symbols introduced in this section are listed in Table 3.

5.1. Block probabilities

The block probability $P_i[ij]$ is the chance that the state at site k , $s_k(t)$, is i and the state at a randomly chosen nearest neighbor is j . Summed block probabilities give frequencies of the elementary states; $P_i[i] = \sum_j P_i[ij]$, where $P_i[i]$ is the global density of sites with state i at time t . $P_i[i]$ need not equal the mean field's $\rho_i(t)$, since the two models have different structure and, hence, different dynamics. We assume spatial symmetry ($P[ij] = P[ji]$), leaving 10 distinct block probabilities. Therefore, the pair-approximation requires nine equations.

5.2. Pair-block transitions

Following Hiebeler (2000), we represent pair-block transitions as:

$$[s_k(t) s_r(t)] \rightarrow [s_k(t+1) s_r(t+1)] \quad r \in \sigma_k. \quad (14)$$

First, consider host birth. Suppose site k is open at time t , so the left side of (14) is a $[0 j]$ pair block. Since we know j , we know the probability that an offspring is dispersed from site r to site k . If a host occupies site r , the probability is b . The transition of a $[0 j]$ pair block *via* birth also depends on the other $(N - 1)$ sites on σ_k whose states are unknown. For a randomly chosen site q on σ_k , other than site r , the conditional probability site q is occupied, given that $s_k(t) = 0$, is $P_t[0h]/P_t[0]$; $h \in \{S, A, V\}$. Each of these $(N - 1)$ sites on σ_k attempts to colonize with probability b times the chance a host occupies the site:

$$b \sum_{h \in \{S, A, V\}} \frac{P_t[0h]}{P_t[0]} = (b/P_t[0])(P_t[0] - P_t[00]). \quad (15)$$

Then the probability, per site of unknown state, of an attempt to colonize an open site k is:

$$\lambda(t) = b \left(1 - \frac{P_t[00]}{P_t[0]} \right). \quad (16)$$

Next, consider avirulent infection in an $[Sj]$ pair block. The probability a susceptible at k is exposed to the avirulent strain at site r is β_a if $j = A$, and 0 otherwise. The conditional probability of an avirulent infection at site q , given a susceptible at k , is $P_t[SA]/P_t[S]$. Then the probability a susceptible at site k is exposed to the avirulent strain from a site q on σ_k is:

$$\theta_A(t) = \beta_A P_t[SA]/P_t[S]. \quad (17)$$

Similarly, the probability that a susceptible is exposed to the virulent strain via contact from site q on σ_k , where the elementary state is unknown, is:

$$\theta_V(t) = \beta_V P_t[SV]/P_t[S]. \quad (18)$$

Given an $[AV]$ pair block, the probability that the avirulently infected host at k is exposed to the virulent strain via the known neighbor is β_v . For each of the $(N - 1)$ sites on σ_k whose states are unknown, the probability of exposure to the virulent strain is:

$$\theta_{si}(t) = \beta_V P_t[AV] / P_t[A]. \quad (19)$$

5.3. Pair-block dynamics

Here we develop two of the pair approximation's equations. Appendix C presents the remaining equations; they use the same transitions explained here, but in different combinations.

First, consider the pair block [0S], where site k is empty and site r is occupied by a susceptible. Eight different $[ij]$ block pairs can become a [0S] pair block in a single period; they have $i \in \{0, S, A, V\}$ and $j \in \{0, S\}$. Then:

$$\begin{aligned} P_{t+1}[0S] = & P_t[00][1 - \lambda(t)]^{N-1} \left(1 - [1 - \lambda(t)]^{N-1} \right) \\ & + \left(1 - (1-b)[1 - \lambda(t)]^{N-1} \right) (\mu_S P_t[S0] + \mu_A P_t[A0] + \mu_V P_t[V0]) \\ & + P_t[0S](1-b)[1 - \lambda(t)]^{N-1} (1 - \mu_S)[1 - \theta_A(t)]^{N-1} [1 - \theta_V(t)]^{N-1} \\ & + [1 - \theta_A(t)]^{N-1} [1 - \theta_V(t)]^{N-1} (1 - \mu_S) (\mu_S P_t[SS] + \mu_A P_t[AS] + \mu_V P_t[VS]). \end{aligned} \quad (20)$$

In the first line of Eq. (20), sites k and r are open. No birth occurs at k , and a birth occurs at r . In the second line k is occupied, and r is open. Mortality occurs at k ; the probability depends on infection status. Birth occurs at r ; the host at k may have dispersed a propagule to r before its death. In the third line k is open, and a susceptible occupies r . No birth occurs at k . The susceptible is not infected by either strain, and survives. In the fourth line k is occupied, and r is occupied by a susceptible. Mortality at k depends on infection status; the susceptible at r avoids infection, and survives. In calculating Eq. (20), $P_t[S0] = P_t[0S]$ by spatial symmetry.

Next, consider the [AV] block pair. Six $[ij]$ block pairs can become an [AV] in a single interval; they have $i \in \{S, A\}$ and $j \in \{S, A, V\}$. The difference equation for the probability of a [AV] block pair is:

$$\begin{aligned}
P_{t+1}[AV] = & \left[[1-\theta_v(t)]^{N-1} + (1-\gamma) \left(1 - [1-\theta_v(t)]^{N-1} \right) \right] \\
& \times \left\{ \begin{aligned} & P_t[SS] (1-\mu_s)^2 (1-[1-\theta_A(t)]^{N-1}) (1-[1-\theta_v(t)]^{N-1}) \left[[1-\theta_A(t)]^{N-1} + \gamma (1-[1-\theta_A(t)]^{N-1}) \right] \\ & + P_t[SA] (1-\mu_s) (1-\mu_A) (1-(1-\beta_A) [1-\theta_A(t)]^{N-1}) \gamma (1-[1-\theta_{si}(t)]^{N-1}) \end{aligned} \right\} \\
& + P_t[SV] (1-\mu_s) (1-\mu_v) (1-[1-\theta_A(t)]^{N-1}) \left[(1-\beta_v) [1-\theta_v(t)]^{N-1} + (1-\gamma) (1-(1-\beta_v) [1-\theta_v(t)]^{N-1}) \right] \\
& + \left[[1-\theta_{si}(t)]^{N-1} + (1-\gamma) \left(1 - [1-\theta_{si}(t)]^{N-1} \right) \right] \\
& \times \left\{ \begin{aligned} & P_t[AS] (1-\mu_A) (1-\mu_s) (1-[1-\theta_v(t)]^{N-1}) \left[(1-\beta_A) [1-\theta_A(t)]^{N-1} + \gamma (1-(1-\beta_A) [1-\theta_A(t)]^{N-1}) \right] \\ & + P_t[AA] (1-\mu_A)^2 \gamma (1-[1-\theta_{si}(t)]^{N-1}) \end{aligned} \right\} \\
& + P_t[AV] (1-\mu_A) (1-\mu_v) \left[(1-\beta_v) [1-\theta_{si}(t)]^{N-1} + (1-\gamma) (1-(1-\beta_v) [1-\theta_{si}(t)]^{N-1}) \right].
\end{aligned} \tag{21}$$

The first pair-block transition in Eq. (21) is $[SS] \rightarrow [AV]$. The susceptible at k must be exposed to avirulent infection; it may avoid exposure to the virulent strain, or may be exposed to both strains with the avirulent winning. The susceptible at r must be exposed to virulent infection. The host at r might avoid exposure to avirulent infection, or might be exposed to both strains simultaneously with the virulent strain winning the host. Then both hosts must survive.

The second block-pair transition in Eq. (21) is $[SA] \rightarrow [AV]$. The susceptible at k must be exposed to avirulent infection. The same host at k might avoid virulent infection, or the avirulent strain may win if the host is exposed to both strains. The avirulently infected host at r must acquire the virulent strain via superinfection. Finally, both hosts must survive. The four other transitions in Eq. (21) are justified similarly.

6. Spatial superinfection: pairwise invasion analysis

We conducted pairwise invasion analyses of both the individual-based, stochastic model and the deterministic pair approximation. Each analysis began with a resident strain at monomorphic, endemic equilibrium. We computed single-strain equilibria for the spatial simulation and pair-approximation models separately. To introduce a competing strain (whether more or less virulent than the resident), we reduced the global density of susceptibles by 0.075. We then converted the corresponding sites (simulation) or pair-block frequencies (pair approximation) to hosts infected by the introduced strain. Hence the initial global density of the invader was held constant across different single-strain equilibria. We recorded invasion of the resident strain whenever the introduced strain's global density exceeded 10^{-3} at time $t = 1000$; otherwise, we recorded that the resident repelled the introduced strain.

The invasion analyses identified any monomorphic singular strategies (Geritz *et al.*, 1998), which we classify according to convergence stability and evolutionary stability. Convergence stability implies that a monomorphic population near a singular strategy can be invaded and excluded by a mutant closer to the singular strategy. Evolutionary stability implies that a singular virulence strategy repels invaders. Following Pugliese (2002a), we term an ESS local if it repels any mutant in a neighborhood around the singular strategy, and global if the ESS repels any feasible mutant. Convergence stability does not guarantee evolutionary stability; neither stability property need imply the other (Geritz *et al.*, 1998). This section divides results according to the two forms assumed for the transmission-virulence ratio, Eqq. (1A) and (1B).

6.1. Transmission/virulence declines as virulence increases

If $\beta(\mu_i) = \mu_i^\alpha/N$ for $\alpha < 1$, increased virulence reduces the ratio of transmission to host-mortality probability. Hence an avirulent strain always has the greater β/μ , implying a potential

“colonization” advantage. A virulent strain has the greater transmission probability, though lower β/μ , and the competitive advantage of superinfection. For this case we report results for two forms of the superinfection function (two values for ψ). We present four invasion analyses and then address quantitative effects of virulence on host densities and mortality frequencies.

6.1.1. Pairwise invasion: strong competitive asymmetry

First we set $\psi = 0.2$, implying a strong competitive asymmetry for given difference in virulence. That is, superinfection occurs relatively frequently for given $(\mu_V - \mu_A)$. Figure 4a shows results for the invasion analysis of the spatially detailed, stochastic model with neighborhood size $N = 48$. Restricting attention to results along the diagonal, we envision evolution *via* sequential replacement of monomorphic populations (Geritz *et al.*, 1998). Selection *via* spatially structured competition in the spatially detailed does not predict evolution to the maximal virulence capable of dynamic persistence, as the mean-field model does. In fact, the pattern indicated a convergent stable, local ESS at the singular strategy μ^* (Fig 4a).

A band of strain coexistence separates strains that invade and exclude the resident from those repelled by the resident. Coexistence implied that each of two strains invaded the other, and the dynamics proceeded to a fixed-point equilibrium.

Figure 4b shows the pairwise invasion plot for this parameter combination’s pair approximation. A convergent stable, local ESS occurred at the singular strategy μ^* , which repels any larger virulence, but can be invaded by sufficiently less virulent mutants (which can then be invaded by a strategy closer to μ^*). Both models indicated that a monomorphic singular strategy may be an evolutionary attractor and exhibit local evolutionary stability, although the pair approximation predicts an ESS virulence exceeding the spatial model’s prediction. Compared to the spatial simulations, the pair approximation predicted that a considerably larger set of paired

strains can coexist. More importantly, a comparison of Figs. 4a and 4b shows clearly that the maximal virulence capable of dynamic, single-strain persistence is smaller for the spatially detailed model than for the pair approximation. The individual-based model appreciates the full impact of spatial clustering of infectives on the dynamics, while the pair approximation relaxes spatial correlations beyond nearest neighbors. These results imply that stronger spatial structuring of the dynamics reduces the maximal virulence capable of persistence and also reduces the evolutionarily stable level of virulence.

6.1.2. *Pairwise invasion: weaker competitive asymmetry*

Setting $\psi = 1.2$ implies a weaker competitive asymmetry between strains. The individual-based model's pairwise-invasion plot, Fig. 5a, suggested a convergent stable, local ESS level of virulence, near the value indicated by simulations with strong competitive asymmetry. Decreasing the advantage of superinfection reduced the extent of strain coexistence in the simulations. Resident strains with low virulence now repelled high-virulence invaders with which they could coexist under greater competitive asymmetry.

The pair approximation's invasion analysis, Fig. 5b, also predicted a convergent and evolutionarily stable level of virulence. The local ESS occurred at a lower virulence, compared to the pair approximation under strong competitive asymmetry. However, the extent of coexistence remained similar. Comparing Figs. 5a and 5b reveals two effects noted under strong competitive asymmetry. Stronger spatial structuring of the dynamics (individual-based model, Fig. 5a) reduces the maximal virulence capable of persisting alone, and reduces the predicted EES level of virulence under pairwise competition.

For parameter values we present, both strong and weak competitive asymmetry predict a monomorphic virulence-strategy exhibiting both convergence stability and local evolutionary

stability. Comparing the levels of competitive asymmetry predicts that increasing the frequency of superinfection (strong asymmetry) may lead to a greater local ESS level of virulence, and may permit increased coexistence of competing strains. Increased competitive asymmetry implies that opportunities for colonization-competition distinctions between avirulent and virulent strains increase. Comparing degrees of spatial structure (simulation *vs.* pair approximation) within either level of competitive asymmetry predicts that increased spatial clustering of infections reduces the locally stable level of virulence.

6.1.3. *Host densities and mortality frequency*

Here we evaluate effects of virulence on host densities. For simplicity, we separate results based competitive exclusion from results on pairwise coexistence. To characterize disease clustering, we plot a local contagion ratio for pathogen infection: the frequency of infected hosts among sites neighboring an infected host divided by the square of the global frequency of infected hosts. In terms of the pair approximation's state variables, the contagion ratio is $P[ii]/(P[i])^2$, where i is an infected-host state ($i = A$ or V). In the absence of local spatial correlation, the ratio will be unity by independence; clustering of infectives yields values exceeding unity (Tainaka and Araki, 1999). We recognize that these are equilibrium values, and the impact of clustering on dynamics may occur soon after the invader's introduction (van Baalen and Rand, 1998).

Figure 6a shows global densities of infected hosts at single-strain equilibrium as a function of virulence. The equilibria were computed for a small neighborhood ($N = 8$) and strong competitive asymmetry ($\psi = 0.2$); densities are plotted for both the spatially detailed model and pair approximation. The same figure also shows the local contagion ratios. Under

both models the density of infected hosts declined as virulence increased; the decline in infectives was accompanied by an increase in the global density of susceptibles (not shown).

For the combination of a small neighborhood and strong competitive asymmetry, global density of infection in the pair approximation always exceeded the simulation's density for the same virulence (although the numerical difference was small at very low virulence). This difference parallels the observation that the spatially detailed dynamics sent the pathogen to extinction at a much lower virulence level than does the pair approximation (Figs 4a and 4b). We anticipated these results qualitatively, since pair approximation underestimates clumping of infection when neighborhoods are small. Figure 6a shows that local contagion ratios uniformly exceeded unity and increased with virulence in both models, and that pair approximation's overestimation of the global density of infection follows from underestimation of the local clustering of infection. For small neighborhoods, pair approximation can miss the degree to which an invading strain's clustering impacts its dynamics (Sato and Iwasa, 2000; Korniss and Caraco, 2005). Although susceptible hosts became more common as virulence increased, the combination of lower infectious-host density and increased relative clumping of infectives strongly constrained the maximal feasible virulence in the spatially detailed model.

Figure 6b plots single-strain, endemic equilibria for a larger neighborhood ($N = 48$, as in the pairwise invasion plots). Comparing the spatial model and its pair approximation, global densities of infected hosts declined similarly as virulence increased. Pair approximation also mimicked the spatial model's local contagion ratios much better at the larger neighborhood size. More importantly, the larger neighborhood increased the maximal dynamically persistent virulence in both models, and slightly increased the equilibrium density of infected hosts for given virulence. Increased neighborhood size diminishes the likelihood that a pathogen kills its

host before finding another to infect (Caraco *et al.*, 1998), and increases the likelihood that a host will find an open site and reproduce before dieing. Although clustering of diseased hosts occurred, the larger neighborhood size diminished the extinction penalty for relatively virulent pathogens. The resulting increase in the maximal feasible virulence, in turn, made coexistence with minimally virulent strains more likely.

We end this section by examining host densities for virulence pairs capable of coexistence. We compare host populations infected by coexisting pathogens to each of the two single-strain equilibria. Neighborhood size is $N = 48$, and competitive asymmetry is strong ($\psi = 0.2$). These values commonly produced coexistence in both the spatially detailed simulations and pair approximation, and the associated invasion plots are similar. As a convenience, we use the results from pair approximation, since boundaries of the coexistence regions are exact.

Total host density sums susceptibles, avirulent infections and virulent infections. If we represent total host density at coexistence equilibrium as $P^*(\mu_a, \mu_v) = P_S^c + P_A^c + P_V^c$, then the total number of deaths per time interval is proportional to $(\mu_S P_S^c + \mu_A P_A^c + \mu_V P_V^c)$. Densities and mortality count for the two single-strain equilibria are defined similarly.

Given that pathogen strains with virulence levels μ_A and μ_V can coexist, global host density most often was greatest in populations infected by the virulent strain alone; see Fig. 7a. The virulent single-strain equilibrium always maximized the density of susceptible hosts, most often minimized density of infected hosts, and the former effect usually dominated. Infection by the avirulent strain alone most often minimized total host density.

The avirulent strain alone almost always maximized the density of infected hosts; as we just noted, the virulent strain alone almost always minimized the global density of infection. These differences affect the global mortality count. Figure 7b shows the equilibrium population

experiencing the greatest number of deaths per time interval, given the three alternatives defined by a coexistence pair. When the difference ($\mu_V - \mu_A$) is relatively large, the mortality density is greatest in a population infected by only the virulent strain. Here, introducing the avirulent strain (taking the system to the fixed point, coexistence equilibrium) would decrease the mortality per time interval, but would also decrease the total host density (from Fig. 7a). When the difference ($\mu_V - \mu_A$) is relatively small, the mortality density is greatest in a population infected by only the avirulent strain. Here, introducing the virulent strain (leading to coexistence) both increased total host density and decreased the global mortality at equilibrium.

The preceding hypothesis assumes that a disease cannot be eliminated from a host population, and that a more virulent infection can displace a less virulent infection within individual hosts. Given our assumptions, introducing a more virulent strain of that disease could sometimes increase total host density, increase the global density of susceptible (healthy) hosts, and decrease the number of deaths per time interval. These results further can depend on our assumption that disease affects only mortality (not fecundity), and on the model's birth-first order of events (Maniatty *et al.*, 1998; Koella and Doebeli, 1999; see Discussion).

6.2. *Transmission/virulence maximal at intermediate virulence*

If $\beta(\mu_i) \propto \mu_i^\alpha (1 - \mu_i)/N$, Eq. (1B), the ratio of transmission probability to virulence can reach a maximum at intermediate host mortality, hence, at intermediate duration of the infectious period. For the lowest-virulence strains, an increase in virulence promotes both colonization capacity and strength as an interference competitor. Highly virulent strains, of course, have low transmission rates and must rely more on superinfection to persist competitively.

In this section we set $\alpha = 1.6$, and restrict attention to strong competitive asymmetry ($\psi = 0.2$). In the associated computations the transmission probability β reached a maximum near $\mu_i = 0.6$, and the transmission-virulence ratio attained a maximum near $\mu_i = 0.35$.

6.2.1. *Pairwise invasion*

Using the “peaked” form of the infection-transmission function, we conducted pairwise invasion analyses with $N = 48$. Figure 8a shows the invasion plot for the individual-based model, and Fig. 8b shows pair-approximation’s results. Both models produced a convergent stable, singular strategy; the deterministic pair approximation exhibited a local ESS. Neither model mimicked the mean-field’s evolution to criticality. As noted above, the inherent difference between the individual-based model’s and pair approximation’s appreciation of spatial clustering affected the results. Both the singular strategy and the maximal virulence capable of single-strain persistence took smaller values in the spatially exact simulations.

Strain coexistence occurred only rarely in simulation. Pair approximation admitted a set of coexisting strategy pairs. The latter invasion plot indicated that dynamical coexistence was largely limited to pairings between strains with large transmission-virulence ratios and the maximally virulent strains. That is, coexistence under pair approximation tended to link the best colonizers and the strongest interference competitors. Examination of the associated pair-block frequencies revealed that that key to coexistence was that the strongest interference competitors (most virulent strains) remained at low global density (due to spatial aggregation), permitting the avirulent strain’s persistence through colonization of susceptibles. This qualitatively parallels results for the first infection-transmission function we studied.

6.2.2. *Infected host densities*

Figure 9a shows global densities of infected hosts at single-strain equilibrium, as a function of virulence, for a small neighborhood ($N = 8$). Densities are plotted for both the spatially detailed model and pair approximation; the figure also shows local contagion ratios for both models. Infected host density peaks at intermediate virulence for each model, approximating the dependence of transmission on virulence. Infectives aggregated spatially, more so in simulation than in the pair approximation's results. Consequently, pair approximation overestimated densities of infected hosts, when compared to the detailed model's results. Figure 9b shows densities of infected hosts and contagion ratios for a larger neighborhood, $N = 48$. The larger neighborhood reduces the degree of clustering and, not surprisingly, the pair approximation better predicts behavior of the spatially detailed model.

7. Discussion

Superinfection models diseases where individual hosts may contact more than one strain of a pathogen, and properties of the more (or most) virulent strain acquired govern the consequences of infection. Martcheva and Thieme (2003) suggest that in humans, superinfection seldom plays a role in the dynamics of micro-parasitic disease (*cf.* Donnenberg and Whittam, 2001), but occurs commonly in macro-parasitic disease.

Our model introduced spatial structure to superinfection dynamics and asked how pathogen virulence might evolve under strain competition. The model's results predict that increased limitation on host-pathogen spatial dispersal increases extinction of highly virulent strains, and reduces the stationary level of virulence that evolves in response to strain competition. The results associate increased spatial clustering of infected hosts with reduced convergent-stable levels of virulence. The model predicts that coexistence of competing strains becomes more likely when one strain has a high transmission to virulence ratio, but is a poor

interference competitor, and the other strain has a low ratio of transmission to virulence, but has an advantage through interference competition.

When pathogen strains compete both between and within hosts, the dynamics of the host-pathogen interaction defines the context for virulence evolution (Ebert and Mangin, 1997; Castillo-Chavez and Velasco-Hernandez, 1998); the outcome of strain competition depends on details of the population dynamics. Models for the superinfection process may assume density-independent host growth in the absence of disease (Levin and Pimentel, 1981), may fix the host population's total density (Nowak and May, 1994; Claessen and DeRoos, 1995), or may include logistic self-regulation in the host dynamics (Pugliese, 2002b). Our model assumes a host population subject to intraspecific competition; a finite number of sites and local clustering combine to produce self-regulation. When the number of hosts (susceptibles plus infectives) is fixed, so that total mortality is always balanced by birth or immigration, the mean-field superinfection dynamics becomes equivalent to models where different species compete implicitly for space, and higher ranked species displace weaker within-patch competitors (Tilman, 1994; Stone, 1995; Kinzig *et al.*, 1999; Adler and Mosquera, 2000).

The combination of spatially structured disease transmission and virulence-dependent superinfection probabilities distinguishes our model. The mean-field approximation allows virulence to evolve to its critical upper bound, but the introduction of spatial structure predicts lower levels of virulence. At a general level, this result agrees with predictions of other disease-transmission models with spatial structure (Claessen and DeRoos, 1995; Haraguchi and Sasaki, 2000; van Baalen, 2002a). At a more detailed level, we found significant effects of spatial structure in both the pair approximation and simulation model. Our results indicate that spatial

structure, and the consequent clustering, constrained the maximal virulence capable of dynamical persistence and reduced the convergent-stable level of virulence.

Recall that the model's neighborhoods are restricted to nearest neighbors, so that infection occurs on a regular network. If we held the number of neighbors per site constant, but randomly selected the interaction neighbors, the contact network would change. Local clustering would diminish, model behavior should move toward mean-field dynamics, and we would predict higher levels of virulence (Boots and Sasaki, 1999; van Baalen, 2002a).

Virulence management usually refers to purposeful modification of infection-transmission rates, so that low-virulence strains might be selectively favored over more virulent pathogens (Ewald, 1994; Dieckmann *et al.*, 2002). Our results point out that ecological management of a diseased host population can, in some situations, take advantage of more virulent strains to reduce mortality and increase global host density. Suppose that disease cannot be cured (our model admits no recovery) in a population at endemic equilibrium, and that we want to reduce total mortality. Management options are limited to introducing a strain that will invade and exclude the resident, or introducing a strain that will coexist with the resident pathogen (Elliot *et al.*, 2002). Given a strictly monotonic increase in transmission with virulence, introducing a strain slightly more virulent than the resident usually will exclude the latter; mortality consequently declines and global host density increases. Similarly, introducing a virulent strain that will coexist with a less virulent resident sometimes can reduce total mortality. For given strain pairs capable of coexistence, the monomorphic avirulent strain almost always minimized total host density. Hence, if the host is a "pest," introducing low-virulence disease may reduce pest density more effectively than would a high-virulence alternative. These patterns in our results depend on model details. In particular, differences in virulence affect only disease

transmission and host mortality; host reproduction does not depend on infection status. If infection alters fecundity, other patterns will likely arise. Furthermore, our discrete-time model must order events for concurrent updating of lattice sites; we allow host reproduction and pathogen transmission to precede mortality. For some models, the difference between discrete and continuous time simulations can be significant (Huberman and Glance, 1993).

Disease virulence can affect fecundity in addition to, or instead of, host mortality (Gandon *et al.*, 2002). Haraguchi and Sasaki (2000) assume that infection sterilizes hosts and also increases their mortality. O’Keefe and Antonovics (2002) let infection reduce fecundity without an impact on mortality. Both models predict that spatial structuring of transmission can reduce virulence, compared to results for homogeneous mixing. A virulent pathogen might reduce host reproduction so low that clustered infectives would not find enough neighboring susceptibles to persist dynamically, an effect paralleling that of disease-induced mortality.

Ewald (1994) defines virulence as increased host mortality caused by infection, and argues that vector-borne diseases are likely to evolve greater virulence than will directly transmitted diseases. The hypothesis supposes that illness renders a host inactive, so that the rate of direct contact with susceptibles will decline as virulence increases. However, the rate of contact with vectors such as flying insects need not decline with virulence. So, direct transmission might constrain virulence evolution through loss of contacts, and vectors could relax this constraint (Day, 2002). In our model’s terms, vector-borne transmission could effectively increase neighborhood size (Caraco *et al.*, 2001) or randomize the contact network, both of which could increase the competitive advantage of virulent pathogen strains.

Antia *et al.* (1994) suppose that more virulent infections generate greater concentrations of parasites within a host’s tissues. Increased within-host parasite density increases the between-

host transmission rate of disease, and may also increase the rate at which the host's immune system produces antigen-specific cells. An increased immune response accelerates the host's recovery, leading to a virulence-modulated tradeoff between transmission rate and duration of the infectious period. If the host's nutritional status is good, an immune response need not tax the host sufficiently to exact a fecundity or survival cost (Roberts *et al.*, 1995). But energetic stress associated with reproduction (Oppliger *et al.*, 1996) or development (Whitaker and Fair, 2002) can result in antagonism between defense against disease and other elements of fitness.

Our analyses assumed the pathogen could evolve through pairwise competition, but held the host constant. Host resistance to infection will sometimes co-evolve with transmission-virulence properties of pathogens (Bowers and Hodgkinson, 2001; Gandon *et al.*, 2002; Holt and Hochberg, 2002). Interactions between horizontal and vertical transmission may also affect virulence evolution (Kover and Clay, 1998; Koella and Doebeli, 1999). Finally, Thomas *et al.* (2000) argue that costs of disease to a host may sometimes be compensated by indirect benefits of parasitism, including avoidance by predators, and (once recovered) demonstration of disease resistance to potential mates.

Appendix A. Transition probabilities for the detailed model

This appendix specifies transition probabilities between a site's elementary states. $s_k(t)$ identifies the elementary state of site k at time t ; $s_k(t) \in \{0, S, A, V\}$. The number of sites on the interaction neighborhood, for both host propagation and infection transmission, is $|\sigma_k| = N$, *i.e.*, the N nearest neighbors of k . $n(s)$ counts the respective elementary states on σ_k at time t . $0 \leq n(s) \leq N$, and $\sum_s n(s) = N$.

Suppose that site k is open at time t . Then $s_k(t+1) \in \{0, S\}$; no change occurs, or a newly produced susceptible occupies the empty site. The probability of a birth at site k is:

$$1 - (1 - b)^{N - n^{(0)}}. \quad (\text{A.1})$$

The complement of (A1) is the probability of no change at an open site.

Next suppose site k is occupied by a susceptible. If $s_k(t) = S$, $s_k(t+1) \in \{0, S, A, V\}$. A susceptible host may acquire an avirulent infection and survive, may acquire a virulent infection and survive, may die, or may avoid infection and survive (no change). The probability that the susceptible is infected by the avirulent strain and survives to $(t+1)$ is:

$$[1 - (1 - \beta_A)^{n^{(A)}}] [(1 - \beta_V)^{n^{(V)}} + [1 - (1 - \beta_V)^{n^{(V)}}] (1 - \gamma)] (1 - \mu_S). \quad (\text{A.2})$$

The probability that a susceptible is virulently infected and survives is:

$$[1 - (1 - \beta_V)^{n^{(V)}}] [(1 - \beta_A)^{n^{(A)}} + [1 - (1 - \beta_A)^{n^{(A)}}] \gamma] (1 - \mu_S). \quad (\text{A.3})$$

A susceptible's mortality probability is μ_S . The probability of no change when $s_k(t) = S$ complements the sum of these three probabilities.

Now suppose that an avirulently infected host occupies site k at time t . If $s_k(t) = A$, then $s_k(t+1) \in \{0, A, V\}$. An avirulently infected host may acquire the virulent strain and survive, may die, or may avoid superinfection and survive. The probability that the virulent strain displaces the avirulent (via superinfection), and the host survives is:

$$[1 - (1 - \beta_V)^{n^{(V)}}] \gamma (1 - \mu_A). \quad (\text{A.4})$$

The mortality probability is μ_A . The probability of no change (*i.e.*, avoiding superinfection and surviving) is the complement of these two probabilities.

Finally, suppose that a virulently infected host occupies site k . If $s_k(t) = V$, then $s_k(t+1) \in \{0, V\}$. The site becomes open through mortality with probability μ_V . The probability of no change is $(1 - \mu_V)$, completing the model's transition probabilities.

Appendix B. Mean-field approximation

The global density of susceptibles at time $(t + 1)$ sums densitie of births at open sites plus susceptibles at time t that avoid both avirulent and virulent infection and then survive. Hence:

$$\rho_S(t+1) = B (\rho_S + \rho_A + \rho_V) \rho_0 + \rho_S(t) \left[1 - \mu_A^\alpha \rho_A(t) \right] \left[1 - \mu_V^\alpha \rho_V(t) \right] (1 - \mu_S). \quad (\text{B.1})$$

The global density of avirulently infected hosts at time $(t + 1)$ has four sources. The avirulent strain, and not the virulent, is transmitted to some susceptibles that survive. Second, both strains are transmitted to some susceptibles, the avirulent strain wins, and the hosts survive. Third, some avirulently infected hosts avoid contacting the virulent strain and survive. Finally, the virulent strain is transmitted to some avirulently infected hosts, but superinfection fails and the hosts survive. Then:

$$\begin{aligned} \rho_A(t+1) = & \rho_S(t) \mu_A^\alpha \rho_A(t) \left[1 - \mu_V^\alpha \rho_V(t) + (1 - \gamma) \mu_V^\alpha \rho_V(t) \right] (1 - \mu_S) \\ & + \rho_A(t) \left[1 - \mu_V^\alpha \rho_V(t) + (1 - \gamma) \mu_V^\alpha \rho_V(t) \right] (1 - \mu_A). \end{aligned} \quad (\text{B.2})$$

The global density of virulently infected hosts at time $(t + 1)$ has four sources. The virulent strain, and not the avirulent, is transmitted to some susceptibles that survive. Second, both strains are transmitted to some susceptibles, the virulent strain wins, and the hosts survive. Third, the virulent strain displaces the avirulent strain *via* superinfection in some hosts that survive; finally, some virulently infected hosts survive. Then:

$$\begin{aligned} \rho_V(t+1) = & \rho_S(t) \mu_V^\alpha \rho_V(t) \left[1 - \mu_A^\alpha \rho_A(t) + \gamma \mu_A^\alpha \rho_A(t) \right] (1 - \mu_S) \\ & + \rho_A(t) \gamma \mu_V^\alpha \rho_V(t) (1 - \mu_A) + \rho_V(t) (1 - \mu_V). \end{aligned} \quad (\text{B.3})$$

After simplification, expressions (B.1) – (B.3) become Eqq. (3) – (5) in the text.

In the absence of disease, $\rho_A(t) = \rho_V(t) = 0$. At positive, disease-free equilibrium:

$\Delta\rho_S(t) = \rho_S(t) (B[1 - \rho_S(t)] - \mu_S)$, so that $\rho_S^* = 1 - \mu_S/B$, for $\mu_S < B$.

If a single pathogen strain, with host-mortality probability $\mu_A > \mu_S$, invades the disease-free equilibrium, the strain's growth rate when rare must exceed unity, requiring:

$$\rho_A(t+1)/\rho_A(t) = (1 + \rho_S^* \mu_A^\alpha) (1 - \mu_S) > 1. \quad (\text{B.4})$$

Substituting for ρ_S^* in the absence of disease and then simplifying yields expression (6) in the text. The same condition results by requiring that the pathogen's reproduction number, R_0 , exceed unity for invasion. Since the mean-field model assumes homogeneous mixing, we have:

$$R_0(\mu_A) = \rho_S^* (1 - \mu_S) \left(\frac{\mu_A^{1-\alpha}}{\mu_A} \right) > 1. \quad (\text{B.5})$$

Since $0 < \alpha < 1$, $\partial R_0/\partial \mu_A < 0$; for homogeneous mixing, growth when rare declines with any increase in virulence. Expression (B.5) shows that for any positive density of susceptibles, there is a transmission to virulence ratio large enough for successful pathogen invasion.

If a single pathogen strain invades the host population and advances to endemic equilibrium, the growth rate in (B.4) falls to unity, and the equilibrium density of susceptible hosts becomes $\rho_S^* = \mu_A^{1-\alpha}/(1 - \mu_S)$. At the single-strain endemic equilibrium the total density of hosts is $\rho^* = \rho_S^* + \rho_A^*$. Host birth and survival balances mortality, and ρ^* satisfies:

$$\rho^* = B \rho^* (1 - \rho^*) + \mu_A^{1-\alpha} + \left(\rho^* - \frac{\mu_A^{1-\alpha}}{1 - \mu_S} \right) (1 - \mu_A). \quad (\text{B.6})$$

Substituting and simplifying yields:

$$B(\rho^*)^2 + (\mu_A - B)\rho^* - \rho_S^*(\mu_A - \mu_S) = 0. \quad (\text{B.7})$$

The root of the quadratic on $(0, 1)$ has the form shown in eq (7) of the text, where $\rho_A^* = \rho^* - \rho_S^*$ at single-strain endemic equilibrium.

Given the single-strain equilibrium, we ask if a second strain can invade. Consider a pair of strains with host-mortality probabilities $\mu_A < \mu_V$. Suppose the avirulent strain is resident; then the equilibrium is given by $\rho_S^* = \mu_A^{1-\alpha} / (1 - \mu_S)$ and by Eq. (7) in the text. The virulent strain advances when rare if its increase through infecting susceptibles and through superinfection exceeds the loss through host mortality; successful invasion by the virulent strain requires:

$$\mu_V^\alpha \rho_S^* (1 - \mu_A^\alpha \rho_A^* [1 - \gamma]) (1 - \mu_S) + \gamma \mu_V^\alpha \rho_A^* (1 - \mu_A) > \mu_V, \quad (\text{B.8})$$

where γ increases with $(\mu_V - \mu_A)$. After simplification, we obtain expression (8) in the text.

Now assume the virulent strain is resident; the endemic equilibrium is described in the text. The avirulent strain advances when rare when:

$$\left[\mu_A^\alpha \rho_S^* (1 - \mu_S) + 1 - \mu_A \right] \left[1 - \mu_V^\alpha \rho_V^* + (1 - \gamma) \mu_V^\alpha \rho_V^* \right] > 1. \quad (\text{B.9})$$

Simplification yields expression (9) in the text.

Appendix C. Pair approximation dynamics

Equations for $P_t[OS]$ and $P_t[AV]$ appear in the text; we present the remaining seven difference equations here. We begin with the $[00]$ block pair. Generating a pair block with two empty sites requires an already empty pair block and no births, no birth and a death on a block with exactly one site occupied, or two deaths on a pair block with both sites occupied. So:

$$\begin{aligned}
P_{t+1}[00] &= P_t[00] [1-\lambda(t)]^{2(N-1)} \\
&+ 2 (\mu_S P_t[0S] + \mu_A P_t[0A] + \mu_V P_t[0V]) (1-b) [1-\lambda(t)]^{N-1} \\
&+ \mu_S^2 P_t[SS] + \mu_A^2 P_t[AA] + \mu_V^2 P_t[VV] + 2 (\mu_S \mu_A P_t[SA] + \mu_S \mu_V P_t[SV] + \mu_A \mu_V P_t[AV]).
\end{aligned} \tag{C.1}$$

Next consider the [0A] block pair. No [i0] block becomes a [0A] block in one time interval, since hosts are born susceptible. No [iV] block becomes an [iA] in a single period, since the avirulent strain cannot displace the virulent. Eight different pair blocks can produce a [0A] block. Any transition of an [iS] to [0A] requires avirulent infection at site r . Any transition of a [iA] block to [0A] requires that the host at site r avoid superinfection. So:

$$\begin{aligned}
P_{t+1}[0A] &= (1-\mu_S) \left(1 - [1-\theta_A(t)]^{N-1}\right) \left[[1-\theta_V(t)]^{N-1} + (1-\gamma) \left(1 - [1-\theta_V(t)]^{N-1}\right) \right] \\
&\quad \times \left((1-b) [1-\lambda(t)]^{N-1} P_t[0S] + \mu_S P_t[SS] \right) \\
&+ P_t[AS] \mu_A (1-\mu_S) \left(1 - (1-\beta_A) [1-\theta_A(t)]^{N-1}\right) \left[[1-\theta_V(t)]^{N-1} + (1-\gamma) \left(1 - [1-\theta_V(t)]^{N-1}\right) \right] \\
&+ P_t[VS] \mu_V (1-\mu_S) \left(1 - [1-\theta_A(t)]^{N-1}\right) \\
&\quad \times \left[(1-\beta_V) [1-\theta_V(t)]^{N-1} + (1-\gamma) \left(1 - (1-\beta_V) [1-\theta_V(t)]^{N-1}\right) \right] \\
&+ (1-\mu_A) \left[[1-\theta_{si}(t)]^{N-1} + (1-\gamma) \left(1 - [1-\theta_{si}(t)]^{N-1}\right) \right] \\
&\quad \times \left((1-b) [1-\lambda(t)]^{N-1} P_t[0A] + \mu_S P_t[SA] + \mu_A P_t[AA] \right) \\
&+ \mu_V (1-\mu_A) P_t[VA] \left[(1-\beta_V) [1-\theta_{si}(t)]^{N-1} + (1-\gamma) \left(1 - (1-\beta_V) [1-\theta_{si}(t)]^{N-1}\right) \right].
\end{aligned} \tag{C.2}$$

The first transition in (C.2) is $[0S] \rightarrow [0A]$. Site k is empty, and no birth occurs there. The susceptible host at site r must be exposed to avirulent infection, and not be infected by the virulent strain. Then the host at r must survive. The three other $[iS] \rightarrow [0A]$ transitions require mortality, rather than birth, at k . Note that in the four $[iA] \rightarrow [0A]$ transitions, the avirulently infected host at site r must avoid superinfection.

Next consider a block with two susceptibles. No block pair that includes an infected host can become an $[SS]$ in a single period, since hosts do not recover. Empty sites require a birth, and susceptibles must avoid infection. So:

$$\begin{aligned}
P_t[SS] = & P_t[00] \left(1 - [1 - \lambda(t)]^{N-1}\right)^2 + (1 - \mu_1)^2 P_t[SS] [1 - \theta_A(t)]^{2(N-1)} [1 - \theta_V(t)]^{2(N-1)} \\
& + 2P_t[0S] (1 - \mu_S) \left(1 - (1 - b) [1 - \lambda(t)]^{N-1}\right) [1 - \theta_A(t)]^{N-1} [1 - \theta_V(t)]^{N-1}.
\end{aligned} \tag{C.3}$$

The 2 in the last term of (C.3) indicates that transitions from a $[0S]$ pair block or from an $[S0]$ block to a $[SS]$ pair block occur with the same probability.

Now consider the $[SA]$ block pair. Since infected hosts do not recover, neither $[Aj]$ nor $[Vj]$ pair blocks become an $[SA]$ block in a single period. The avirulent strain cannot displace the virulent hosts, so no $[iV]$ block becomes an $[SA]$ block in a single period. That leaves four $[ij]$ block pairs, with $i \in \{0, S\}$ and $j \in \{S, A\}$ in the equation for the $[SA]$ block pair:

$$\begin{aligned}
P_t[SA] = & (1 - \mu_S) P_t[OS] \left(1 - (1 - b) [1 - \lambda(t)]^{N-1}\right) \\
& \times \left(1 - [1 - \theta_A(t)]^{N-1}\right) \left[[1 - \theta_V(t)]^{N-1} + (1 - \gamma) \left(1 - [1 - \theta_V(t)]^{N-1}\right)\right] \\
& + (1 - \mu_A) P_t[OA] \left(1 - (1 - b) [1 - \lambda(t)]^{N-1}\right) \left[[1 - \theta_{si}(t)]^{N-1} + (1 - \gamma) \left(1 - [1 - \theta_{si}(t)]^{N-1}\right)\right] \\
& + (1 - \mu_S)^2 P_t[SS] [1 - \theta_A(t)]^{N-1} [1 - \theta_V(t)]^{N-1} \\
& \times \left(1 - [1 - \theta_A(t)]^{N-1}\right) \left[[1 - \theta_V(t)]^{N-1} + (1 - \gamma) \left(1 - [1 - \theta_V(t)]^{N-1}\right)\right] \\
& + (1 - \mu_S)(1 - \mu_A) P_t[SA] \\
& \times (1 - \beta_A) [1 - \theta_A(t)]^{N-1} [1 - \theta_V(t)]^{N-1} \left[[1 - \theta_{si}(t)]^{N-1} + (1 - \gamma) \left(1 - [1 - \theta_{si}(t)]^{N-1}\right)\right]
\end{aligned} \tag{C.4}$$

The $[iS]$ blocks must avoid virulent infection, and the $[iA]$ blocks must avoid superinfection to generate the $[SA]$ block pair.

Next consider $[SV]$ block pairs. Since hosts are born susceptible and do not recover once infected, no $[i0]$, $[Aj]$, nor $[Vj]$ block pair can become an $[SV]$ block in a single time period. Six different block pairs are included in the equation for the $[SV]$ block:

$$\begin{aligned}
P_t[SV] &= (1 - (1-b)[1-\lambda(t)]^{N-1}) \\
&\times \left\{ \begin{aligned} &(1-\mu_s) P_t[0S] (1-[1-\theta_v(t)]^{N-1}) \left[[1-\theta_A(t)]^{N-1} + \gamma (1-[1-\theta_A(t)]^{N-1}) \right] \\ &+ (1-\mu_A) P_t[0A] \gamma (1-[1-\theta_{si}(t)]^{N-1}) + (1-\mu_v) P_t[0V] \end{aligned} \right\} \\
&+ (1-\mu_s) [1-\theta_A(t)]^{N-1} [1-\theta_v(t)]^{N-1}
\end{aligned} \tag{C.5}$$

$$\times \left\{ \begin{aligned} &(1-\mu_s) P_t[SS] (1-[1-\theta_v(t)]^{N-1}) \left[[1-\theta_A(t)]^{N-1} + \gamma (1-[1-\theta_A(t)]^{N-1}) \right] \\ &+ (1-\mu_A) P_t[SA] (1-\beta_A) \gamma (1-[1-\theta_{si}(t)]^{N-1}) + (1-\mu_v) P_t[SV] (1-\beta_v) \end{aligned} \right\}$$

The [0j] blocks with r occupied require a birth at site k ; [0A] also requires superinfection at site r .

Now consider the [AA] block pair. Pair blocks including either an open site or a virulently infected host cannot become a [AA] block in a single interval. For the [AA] block:

$$\begin{aligned}
P_t[AA] &= (1-\mu_s)^2 P_t[SS] (1-[1-\theta_A(t)]^{N-1})^2 \left[[1-\theta_v(t)]^{N-1} + (1-\gamma) (1-[1-\theta_v(t)]^{N-1}) \right]^2 \\
&+ 2 (1-\mu_s) (1-\mu_A) P_t[SA] (1-(1-\beta_A) [1-\theta_A(t)]^{N-1}) \\
&\quad \times \left[[1-\theta_v(t)]^{N-1} + (1-\gamma) (1-[1-\theta_v(t)]^{N-1}) \right] \left[[1-\theta_{si}(t)]^{N-1} + (1-\gamma) (1-[1-\theta_{si}(t)]^{N-1}) \right] \\
&+ (1-\mu_A)^2 P_t[AA] \left[[1-\theta_{si}(t)]^{N-1} + (1-\gamma) (1-[1-\theta_{si}(t)]^{N-1}) \right]^2.
\end{aligned} \tag{C.6}$$

The 2 associated with the [SA] pair block in (C.6) indicates that both an [SA] block and an [AS] block are changed to [AA] by the same transitions.

Finally, consider the [VV] pair block. Any block without an open site can become a [VV] block pair in a single time period. So:

$$\begin{aligned}
P_t[VV] &= \left[[1-\theta_A(t)]^{N-1} + \gamma \left(1 - [1-\theta_A(t)]^{N-1} \right) \right] \\
&\quad \times \left\{ \begin{aligned} &(1-\mu_S)^2 P_t[SS] \left(1 - [1-\theta_V(t)]^{N-1} \right)^2 \left[[1-\theta_A(t)]^{N-1} + \gamma \left(1 - [1-\theta_A(t)]^{N-1} \right) \right] \\ &+ 2(1-\mu_S)(1-\mu_V) P_t[SV] \left(1 - (1-\beta_V) [1-\theta_V(t)]^{N-1} \right) \end{aligned} \right\} \\
&+ 2(1-\mu_S)(1-\mu_A) P_t[SA] \left(1 - [1-\theta_V(t)]^{N-1} \right) \\
&\quad \times \left[(1-\beta_A) [1-\theta_A(t)]^{N-1} + \gamma \left(1 - (1-\beta_A) [1-\theta_A(t)]^{N-1} \right) \right] \gamma \left(1 - [1-\theta_{si}(t)]^{N-1} \right) \\
&+ (1-\mu_A)^2 P_t[AA] \left[\gamma \left(1 - [1-\theta_{si}(t)]^{N-1} \right) \right]^2 \\
&+ 2 P_t[AV] (1-\mu_A) (1-\mu_V) \gamma \left(1 - (1-\beta_V) [1-\theta_{si}(t)]^{N-1} \right) + (1-\mu_V)^2 P_t[VV].
\end{aligned} \tag{C.7}$$

Eqq. (20) and (21) and Eqq. (C.1) through (C.7) complete the pair-approximation model.

Acknowledgements

This material is based upon work supported by the National Science Foundation under Grant No. 0342689 (T. Caraco and G. Korniss). Each of three reviewers provided insightful comments and useful criticisms that improved the paper significantly, and we thank them. We also appreciate discussion with I. N. Wang.

References

- Adler, F.R., Mosquera, J., 2000. Competition, biodiversity, and analytic functions in spatially structured habitats. *Ecology* 81, 3226–3232.
- Antia, R., Levin, B.R., May, R.M., 1994. Within-host population dynamics and the evolution and maintenance of microparasite virulence. *Amer. Naturalist* 144, 457–472.
- Boots, M., Sasaki, A., 1999. 'Small worlds' and the evolution of virulence: Infection occurs locally and at a distance. *Proc. R. Soc. London B* 266, 1933-1938.
- Bowers, R. G., Hodgkinson, D.E., 2001. Community dynamics, trade-offs, invasion criteria and the evolution of host resistance to microparasites. *J. Theoret. Biol.* 212, 315–331.
- Bremermann, H.J., Pickering, J., 1983. A game-theoretical model of parasite virulence. *J. Theoret. Biol.* 100, 411–426.
- Bremermann, H., Thieme, H., 1989. A competitive exclusion principle for pathogen virulence. *J. Math. Biol.* 27, 179-190.
- Bryant, C., Behm, C., 1989. *Biochemical Adaptation in Parasites*. Chapman & hall, London.
- Bull, J.J., 1994. Virulence. *Evolution* 48, 1423–1437.
- Caraco, T., Duryea, M., Gardner, G., Maniatty, W., Szymanski, B.K., 1998. Host spatial heterogeneity and extinction of an SIS epidemic. *J. Theoret. Biol.* **192**, 351-361.
- Caraco, T., Duryea, M.C., Glavanakov, S., Maniatty, W., Szymanski, B.K., 2001. Host spatial heterogeneity and the spread of vector-borne infection. *Theoret. Population Biol.* 59, 185-206.
- Castillo-Chavez, C., Velasco-Hernandez, J.X., 1998. On the relationship between tight

- coevolution and superinfection. *J. Theoret. Biol.* 192, 437-444.
- Claessen, D., de Roos, A.M., 1995. Evolution of virulence in a host-pathogen system with local pathogen transmission. *Oikos* 74, 401-413.
- Day, T., 2002. The evolution of virulence in vector-borne and directly transmitted parasites. *Theoret. Population Biol.* 62, 199-213.
- Dieckmann, U., Metz, J.A.J., Sabelis, M. W., Sigmund, K., Law, R., Metz, H. (Eds.), 2002. *Adaptive Dynamics of Infectious diseases: In Pursuit of Virulence Management*. Cambridge University Press, Cambridge.
- Donnenberg, M.S., Whittam, T.S., 2001. Pathogenesis and evolution of virulence in enteropathogenic and enterohemorrhagic *Escherichia coli*. *J. Clin. Invest.* 107, 539-548.
- Duryea, M., Caraco, T., Gardner, G., Maniatty, W., Szymanski, B.K., 1999. Population dispersion and equilibrium infection frequency in a spatial epidemic. *Physica D* 132, 511-519.
- Ebert, D., Mangin, K.L., 1997. The influence of host demography on the evolution of virulence of a microsporidian gut parasite. *Evolution* 51, 1828-1837.
- Elliot, S.L., Sabelis, M.W., Adler, F.R., 2002. Virulence management in biocontrol agents. In: Dieckmann, U., Metz, J.A.J., Sabelis, M. W., Sigmund, K., Law, R., Metz, H. (Eds.) *Adaptive Dynamics of Infectious Diseases: In Pursuit of Virulence Management*. Cambridge University Press, Cambridge, pp. 448-459.
- Ewald, P. W., 1983. Host-parasite relations, vectors, and the evolution of disease severity. *Ann. Rev. Ecol. Syst.* 14, 465-485.
- Ewald, P. W., 1994. *Evolution of Infectious Diseases*. Oxford Univ. Press, Oxford, UK.
- Frank, S.A., 1996. Models of parasite virulence. *Quart. Rev. Biol.* 71, 37-78.

- Gandon, S., van Baalen, M., Jansen, V.A.A., 2002. The evolution of parasite virulence, superinfection and host resistance. *Amer. Naturalist* 159, 658–669.
- Ganusov, V.V., Antia, R., 2003. Trade-offs and the evolution of virulence of microparasites: do details matter? *Theoret. Population Biol.* 64, 211-220.
- Geritz, S.A.H., Kisdi, E., Meszéna G., Metz, J.A.J., 1998. Evolutionarily singular strategies and the adaptive growth and branching of the evolutionary tree. *Evol. Ecol.* **12**, 35–57.
- Haraguchi, Y., Sasaki, A., 2000. The evolution of parasite virulence and transmission rate in a spatially structured population. *J. Theoret. Biol.* 203, 85–96.
- Herre, E.A., 1993. Population structure and the evolution of virulence in nematode parasites of fig wasps. *Science* 259, 1442–1445.
- Hiebeler, D., 2000. Populations on fragmented landscapes with spatially structured heterogeneities: landscape generation and local dispersal. *Ecology* 81, 1629–1641.
- Holt, R.D., Hochberg, M.E., 2002. Virulence on the edge: a source-sink perspective. In: Dieckmann, U., Metz, J.A.J., Sabelis, M. W., Sigmund, K., Law, R., Metz, H. (Eds.), *Adaptive Dynamics of Infectious Diseases: In Pursuit of Virulence Management*, Cambridge University Press, Cambridge, pp. 104-119.
- Hood, M.E., 2003. Dynamics of multiple infection and within-host competition by the anther-smut pathogen. *Amer. Naturalist* 162, 122-133.
- Huberman, B.A., Glance, N.S., 1993. Evolutionary games and computer simulations. *Proc. Natl. Acad. Sci. USA* 90, 7716-7718.
- Ives, A.R., Turner, M.G., Pearson, S.M., 1998. Local explanations of landscape

- patterns: can analytical approaches approximate simulation models of spatial processes?
Ecosystems 1, 35-51.
- Keeling, M.J., 1999. The effects of local spatial structure on epidemiological invasions. Proc. R. Soc. London B 266, 859-867.
- Kinzig, A.P., Levin, S.A., Dushoff, J., Pacala, S., 1999. Limiting similarity, species packing, and system stability for hierarchical competition-colonization models. Amer. Naturalist 153, 371-383.
- Kisdi, E., Meszéna, G., 1993. Density dependent life history evolution in fluctuating environments. In: Yoshimura, J., Clark, C. (Eds.), Adaptation in a Stochastic Environment. Lecture Notes in Biomathematics, Vol. 98, Springer-Verlag, New York, pp. 26-62.
- Koella, J.C., Doebeli, M., 1999. Population dynamics and the evolution of virulence in epidemiological models with discrete host generations. J. Theoret. Biol. 198, 461-475.
- Korniss, G., Caraco, T., 2005. Spatial dynamics of invasion: the geometry of introduced species. J. Theoret. Biol., 233, 137-150.
- Kover, P.X., Clay, K., 1998. Trade-off between virulence and vertical transmission and the maintenance of a virulent plant pathogen. Amer. Naturalist 152, 165-175.
- Levin, S.A., Pimentel, D., 1981. Selection for intermediate rates of increase in parasite-host systems. Amer. Naturalist 117, 308-315.
- Mágori, K., Szabó, P., Mizera, F., Meszéna G., 2005. Adaptive dynamics on a lattice: role of spatiality in competition, co-existence and evolutionary branching. Evol. Ecol. Res. 7, 1-21.
- Maniatty, W., Szymanski, B.K., Caraco, T., 1998. High-performance simulation of

- evolutionary aspects of epidemics. In: Proceedings of the PARA98 Workshop on Applied Parallel Computing in Large Scale Industrial and Scientific Problems, Lecture Notes in Computer Science, Springer-Verlag, Berlin, pp. 322 – 331.
- Martcheva, M., Thieme, H.R., 2003. Progression age enhanced backward bifurcation in an epidemic model with super-infection. *J. Math. Biol.* 46, 385-424.
- Matsuda, H.N., Ogita, A., Sasaki, A., Sato, K., 1992. Statistical mechanics of population: The lattice Lotka-Volterra model. *Prog. Theoret. Physics* 88, 1035–1049.
- May, R.M., Nowak, M., 1995. Coinfection and the evolution of parasite virulence. *Proc. R. Soc. London B* 261, 209–215.
- Mosquera, J., Adler, F.R., 1998. Evolution of virulence: a unified framework for coinfection and superinfection. *J. Theoret. Biol.* 195, 295-313.
- Nakamura, M., Matsuda, H., Iwasa, Y., 1997. The evolution of cooperation in a lattice-structured population. *J. Theoret. Biol.* 184, 65-81.
- Nowak, M.A., May, R.M., 1994. Superinfection and the evolution of parasite virulence. *Proc. R. Soc. London B* 255, 81–89.
- O'Keefe, K.J., Antonovics, J., 2002. Playing by different rules: the evolution of virulence in sterilizing pathogens. *Amer. Naturalist.* 159, 597-605.
- Oppliger, A., Christe, P., Richner, H., 1996. Clutch size and malaria resistance. *Nature* 381, 565.
- Powell, P.D., DeMartini, J.C., Azari, P., Stargell, A., Cordain, L., Tucker, A., 2000. Evolutionary stable strategy: a test of theories for retroviral pathology which are based upon the concept of molecular mimicry. *J. Theoret. Biol.* 202, 213-229.
- Pugliese, A., 2002a. On the evolutionary coexistence of parasite strains. *Math. Biosci.*

177 & 178, 355-375.

- Pugliese, A., 2002b. Virulence evolution in macro-parasites. In: Castillo-Chavez C., Blower S., Kirschner D., Van Den Driessche P., Yakubu A. (Eds.), *Mathematical Approaches for Emerging and Reemerging Infectious Diseases: Models, Methods and Theory*, Part 2, IMA Series Vol. 126, Springer-Verlag, New York, pp. 193-213.
- Rand, D.A., Keeling, M., Wilson, H.B., 1995. Invasion, stability and evolution to criticality in spatially extended, artificial host-pathogen ecologies. *Proc. R. Soc. London B* 259, 55-63.
- Rand, D.A., 1999. Correlation equations and pair approximations for spatial ecologies. In: McGlade, J. M. (Ed.), *Advanced Theoretical Ecology: Principles and Applications*. Blackwell, Oxford, UK, pp. 100-142.
- Roberts, M.G., Smith, G., Grenfell, B.T., 1995. Mathematical models for macroparasites. In: Grenfell, B.T., Dobson, A.P. (Eds.), *Ecology of Infectious Diseases in Natural Populations*, Cambridge University Press, Cambridge.
- Saldaña, J., Santiago, F.E., Solé, R.V., 2003. Coinfection and superinfection in RNA virus populations: a selection-mutation model. *Math. Biosci.* 183, 135-160.
- Sato, K., Matsuda, H., Sasaki, A., 1994. Pathogen invasion and host extinction in lattice structured populations. *J. Math. Biol.* 32, 251-268.
- Sato, K., Iwasa, Y., 2000. Pair approximations for lattice-based ecological models. In: Dieckmann, U., Law, R., Metz, J.A.J. (Eds.), *The Geometry of Ecological Interactions*. Cambridge University Press, Cambridge, pp. 341-358.
- Stone, L., 1995. Biodiversity and habitat destruction: a comparative study of model forest and coral reef ecosystems. *Proc. R. Soc. London B* 261, 381-388.

- Tainaka, K.-I., Araki, N., 1999. Press perturbation in lattice ecosystems: parity law and optimum strategy. *J. Theoret. Biol.* 197, 1-13.
- Thomas, F., Poulin, R., Guégan, J.F., Michalakis, Y., Renaud, F., 2000. Are there pros as well as cons of being parasitized? *Parasit. Today* 16, 533-536.
- Tilman, D., 1994. Competition and biodiversity in spatially structured habitats. *Ecology* 75, 2-16.
- van Baalen, M., 2000. Pair approximations for different spatial geometries. In: Dieckmann, U., Law, R., Metz, J.A.J. (Eds.), *The Geometry of Ecological Interactions*. Cambridge University Press, Cambridge, pp. 359-387.
- van Baalen, M., 2002a. Contact networks and the evolution of virulence. In: Dieckmann, U., Metz, J.A.J., Sabelis, M. W., Sigmund, K., Law, R., Metz, H. (Eds.), *Adaptive Dynamics of Infectious Diseases: In Pursuit of Virulence Management*. Cambridge University Press, Cambridge, pp. 85-103.
- van Baalen, M., 2002b. Dilemmas in virulence management. In: Dieckmann, U., Metz, J.A.J., Sabelis, M. W., Sigmund, K., Law, R., Metz, H. (Eds.), *Adaptive Dynamics of Infectious Diseases: In Pursuit of Virulence Management*. Cambridge University Press, Cambridge, pp. 60-69.
- van Baalen, M., Rand, D.A., 1998. The unit of selection in viscous populations and the evolution of altruism. *J. Theoret. Biol.* 193, 631-648.
- van Baalen, M., Sabelis, M. W., 1995. The dynamics of multiple infection and the evolution of virulence. *Amer. Naturalist* 146, 881-910.
- Whitaker, S., Fair, J., 2002. The costs of immunological challenge to developing mountain chickadees, *Poecile gambeli*, in the wild. *Oikos* 99, 161-165.

Figure Legends

FIG. 1. Feasible transitions between a site's elementary states.

State 0 represents an empty site, state S represents a susceptible host, state A represents avirulent infection, and state V represents virulent infection. Infected hosts do not recover the susceptible state; the transition from state A to state V represents superinfection; the more virulent strain displaces the avirulent strain. Transitions into state 0 represent mortality.

FIG. 2. Pathogen-transmission probabilities.

Plots of $\beta_i(\mu_i)$; thick curve is Eq (1A), and thin curve is Eq (1B). Ordinate is probability pathogen transmitted from given infected host to nearest-neighboring site. Parameter values for Eq (1A) are $\alpha = 0.5$ and $N = 48$. Parameter values for Eq (1B) are $\alpha = 1.6$, $z = 6.245$, and $N = 48$.

FIG. 3. Pairwise invasion analysis of mean-field approximation.

Abscissa is host mortality probability of the resident pathogen at single-strain equilibrium. Ordinate is host mortality due to infection by introduced strain. Below the diagonal, the introduced strain is less virulent than the resident; above the diagonal, the introduced strain is more virulent than the resident. Black indicates that invader advanced and excluded the resident. White indicates that resident repelled invader; latter went extinct. Gray indicates coexistence; invasion succeeded and both strains remained extant. Parameter values are $\alpha = 0.5$, $\psi = 0.2$ (strong competitive asymmetry), and $\mu_S = 0.05$. All entries just above the diagonal are black; hence any resident can be invaded and excluded by a slightly more virulent invader, until virulence reaches the critical upper bound for persistence. Coexistence is largely limited to pairing of strains with virulence less than 0.25 and strains with virulence exceeding 0.5.

FIG. 4. Pairwise invasion analysis: $N = 48$, strong competitive asymmetry.

Transmission/virulence declines monotonically with virulence. Colors defined in legend for Fig. 3. Parameter values are $\alpha = 0.5$, $\psi = 0.2$, and $\mu_S = 0.05$. (a) Spatially detailed model. Each entry is the result of a single simulation. (b) Pair approximation. Stationary virulence strategy μ^* located by considering results along diagonal. Below μ^* we have black over white, so small increase in virulence favored in strain competition. Above μ^* we have white over black, so strain competition favors slightly less virulent strain. Convergent stable stationary point μ^* , with virulence close to 0.6, is a local ESS.

FIG. 5. Pairwise invasion analysis: $N = 48$, weak competitive asymmetry.

Transmission/virulence declines monotonically with virulence. Colors defined in legend for Fig. 3. Parameter values are the same as in Fig. 4, but here $\psi = 0.2$. (a) Spatially detailed model. Each entry is the result of a single simulation. Probability of superinfection reduced in comparison to Fig. 4a; extent of coexistence lower than in Fig. 4a. (b) Pair approximation. Frequency of superinfection reduced in comparison to Fig. 4b. Stationary point μ^* , with virulence close to 0.56, is convergent stable and a local ESS.

FIG. 6. Infected host density at single-strain equilibrium: strong asymmetry,

transmission/virulence declines monotonically with virulence.

Global infection shows density of infected hosts as function of host mortality probability; results of both spatially detailed model (open triangles) and pair approximation (closed squares) plotted. Equilibrium density of infection declines as virulence increases. Local contagion ratio exceeds unity when infected hosts are aggregated spatially; results of both spatially detailed model (closed circles) and pair approximation (open circles) plotted. Parameter values are $\alpha = 0.5$, $\psi = 0.2$, and $\mu_S = 0.05$. (a) Small interaction neighborhood, $N = 8$. (b) Large interaction

neighborhood, $N = 48$. Note improvement of pair approximation with respect to global density of infection.

FIG. 7. Maximal host density and maximal host mortality.

Results from pair approximation with $N = 48$, strong competitive asymmetry, and transmission/virulence declining strictly monotonically in virulence. That is, parameter values are $\alpha = 0.5$, $\psi = 0.2$, and $\mu_S = 0.05$. (a) Pathogen strain(s) maximizing total host density at endemic equilibrium. Given that two strains can coexist, A indicates maximal host density when only avirulent strain infects hosts. V indicates maximal host density when only virulent strain infects hosts, and C indicates maximal host density when both strains occur together. (b) Pathogen strain(s) maximizing host mortality at endemic equilibrium. Given that two strains can coexist, A indicates maximal host mortality when only avirulent strain infects hosts. V indicates maximal host mortality when only virulent strain infects hosts, and C indicates maximal host mortality when both strains occur together.

FIG. 8. Pairwise invasion analysis: $N = 48$, strong competitive asymmetry, transmission/virulence peaks at intermediate virulence.

Colors defined in legend for Fig. 3. Parameter values are $\alpha = 1.6$, $f = 6.254$, $\psi = 0.2$, and $\mu_S = 0.05$. (a) Spatially detailed model. Each entry is the result of a single simulation. (b) Pair approximation. Convergent stable stationary point μ^* , near 0.76, is a local ESS.

FIG. 9. Infected host density at single-strain equilibrium: strong asymmetry, transmission/virulence peaks at intermediate virulence.

Symbols defined in legend for Fig. 6. Parameter values are $\alpha = 1.6$, $f = 6.254$, $\psi = 0.2$, and $\mu_S = 0.05$. Global infection shows density of infected hosts as function of host mortality probability; results of both spatially detailed model and pair approximation plotted. Equilibrium density of

infection varies nonlinearly with virulence. Local contagion ratio exceeds unity when infected hosts are aggregated spatially; results of both spatially detailed model and pair approximation plotted. (a) $N = 8$. (b) $N = 48$. Pair approximation better predicts infected host density with larger neighborhood. Note difference of scale for contagion ratio.

Fig. 1

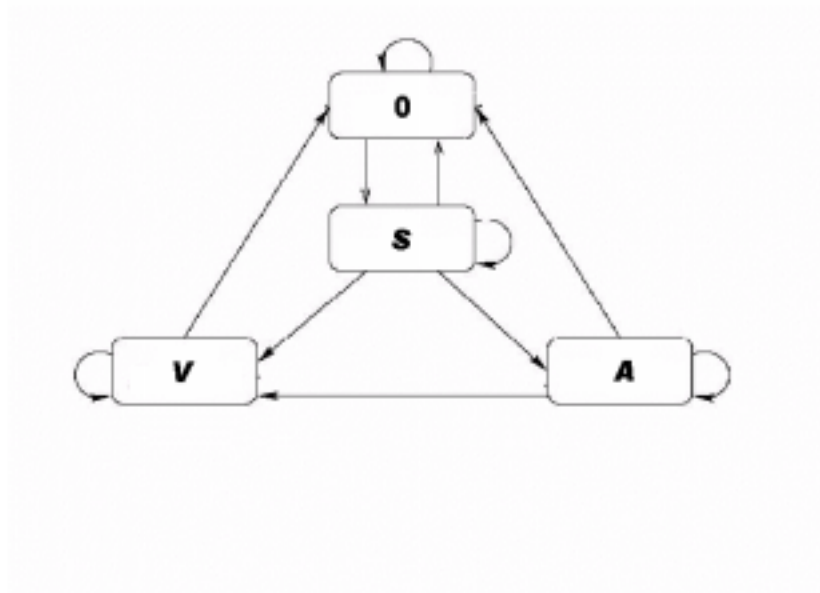


Fig. 2

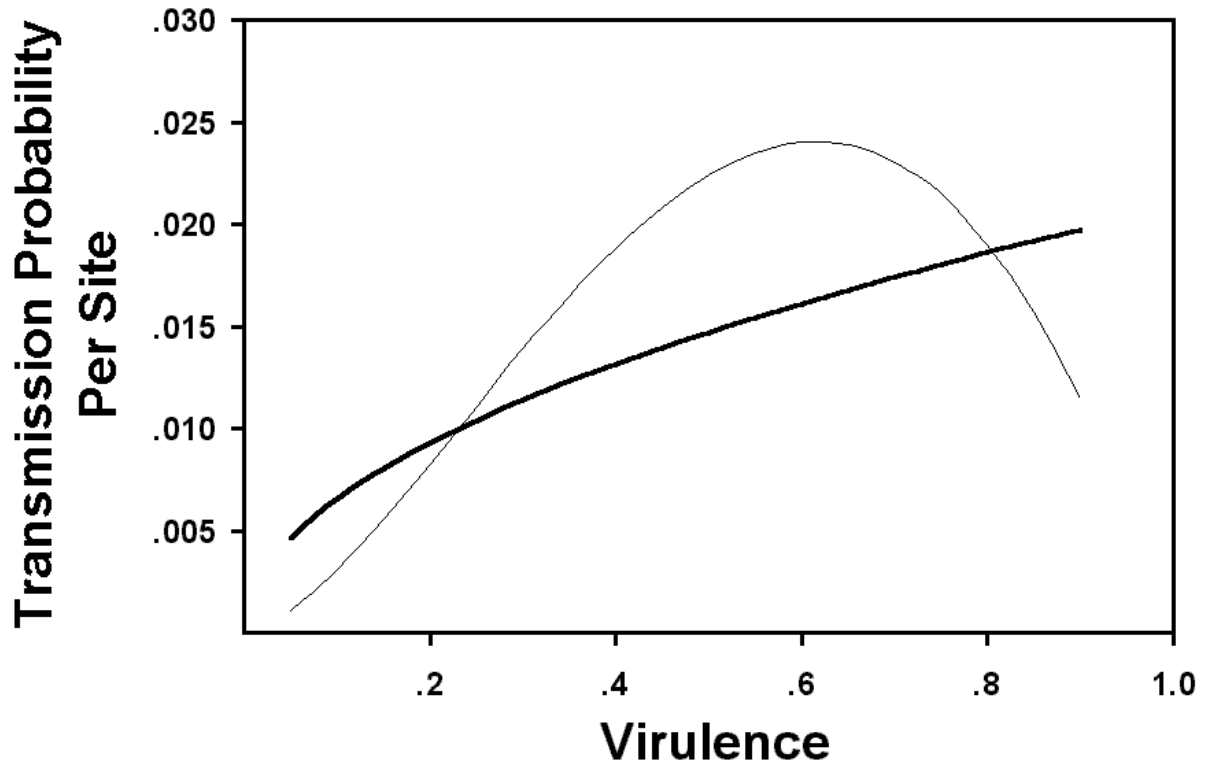


Fig. 3

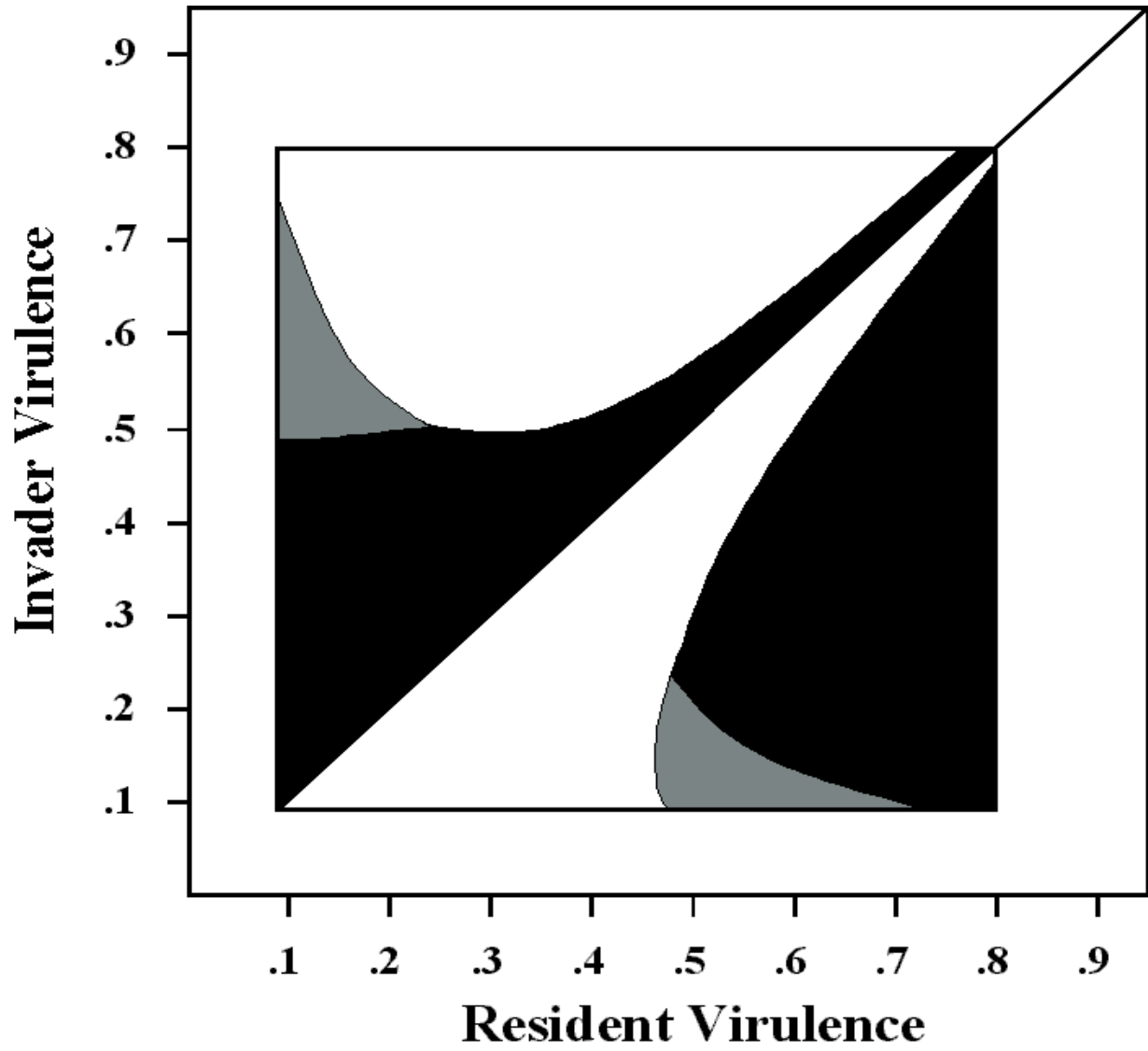


Fig. 4

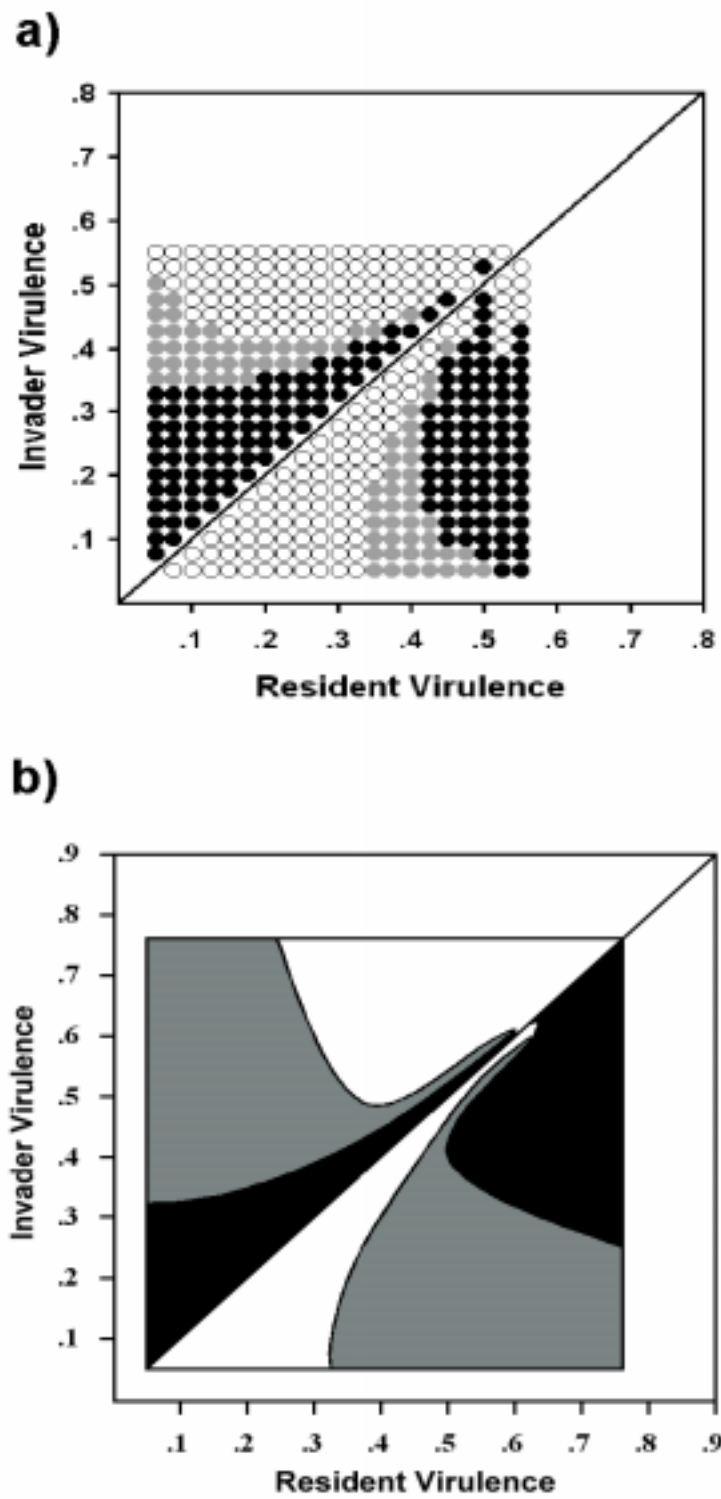


Fig. 5

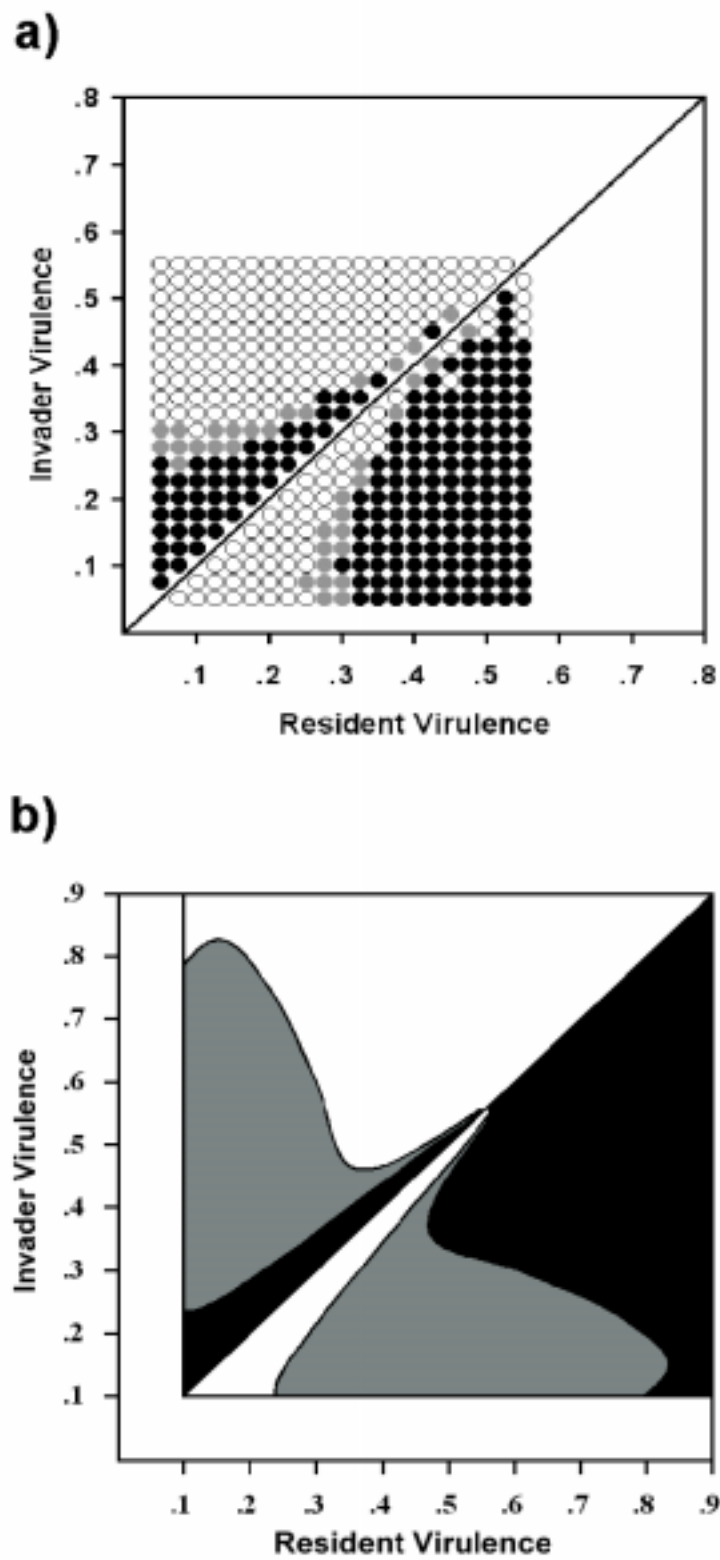


Fig. 6

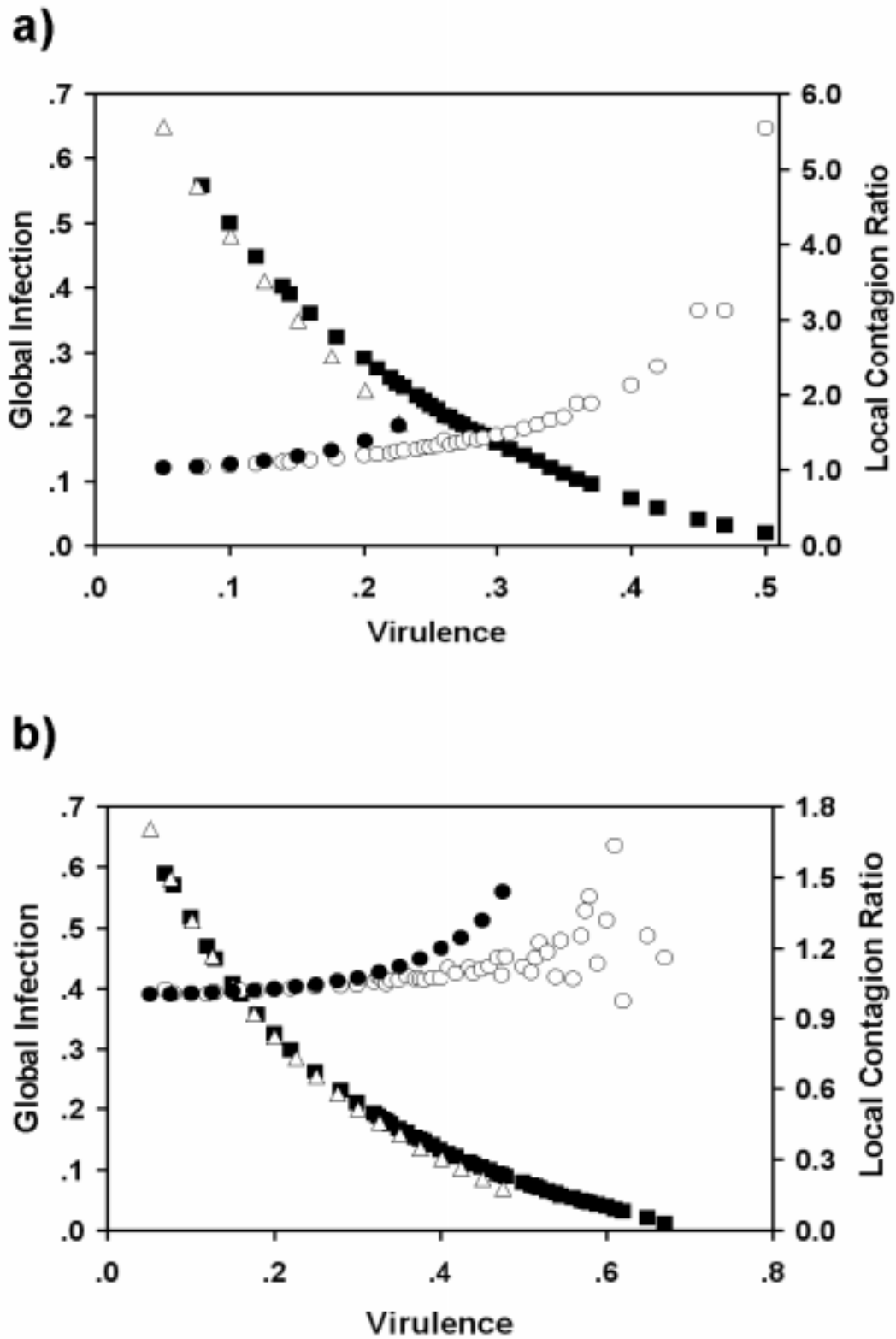


Fig. 7

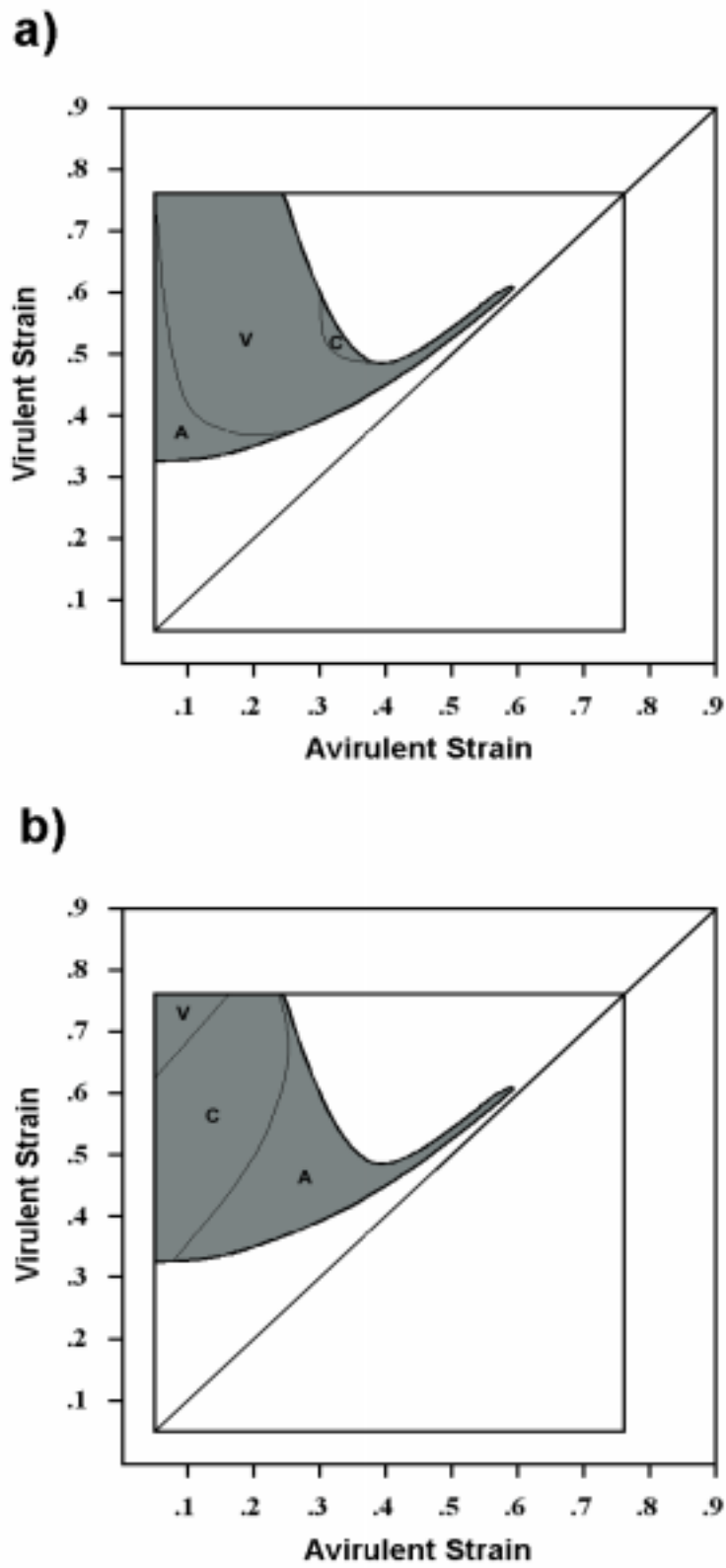


Fig. 8

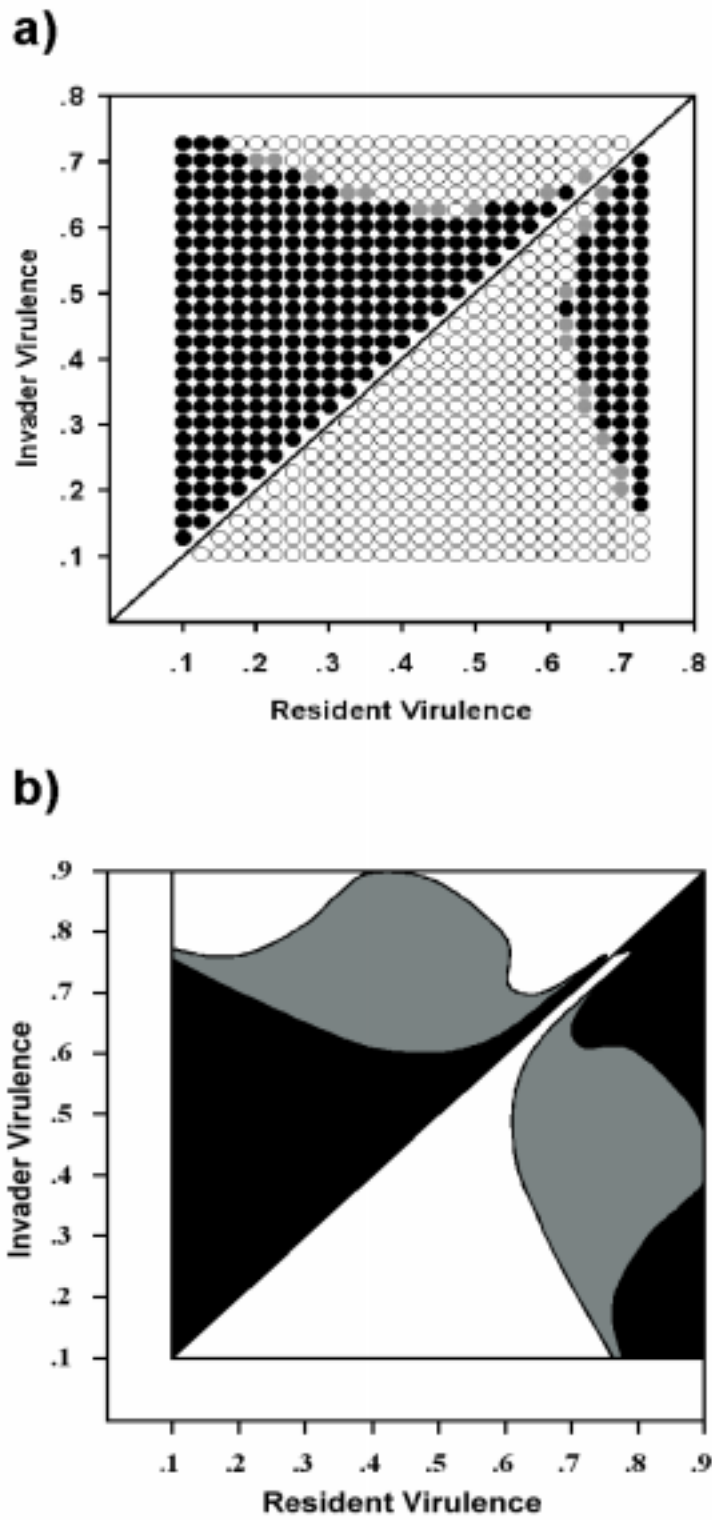


Fig. 9

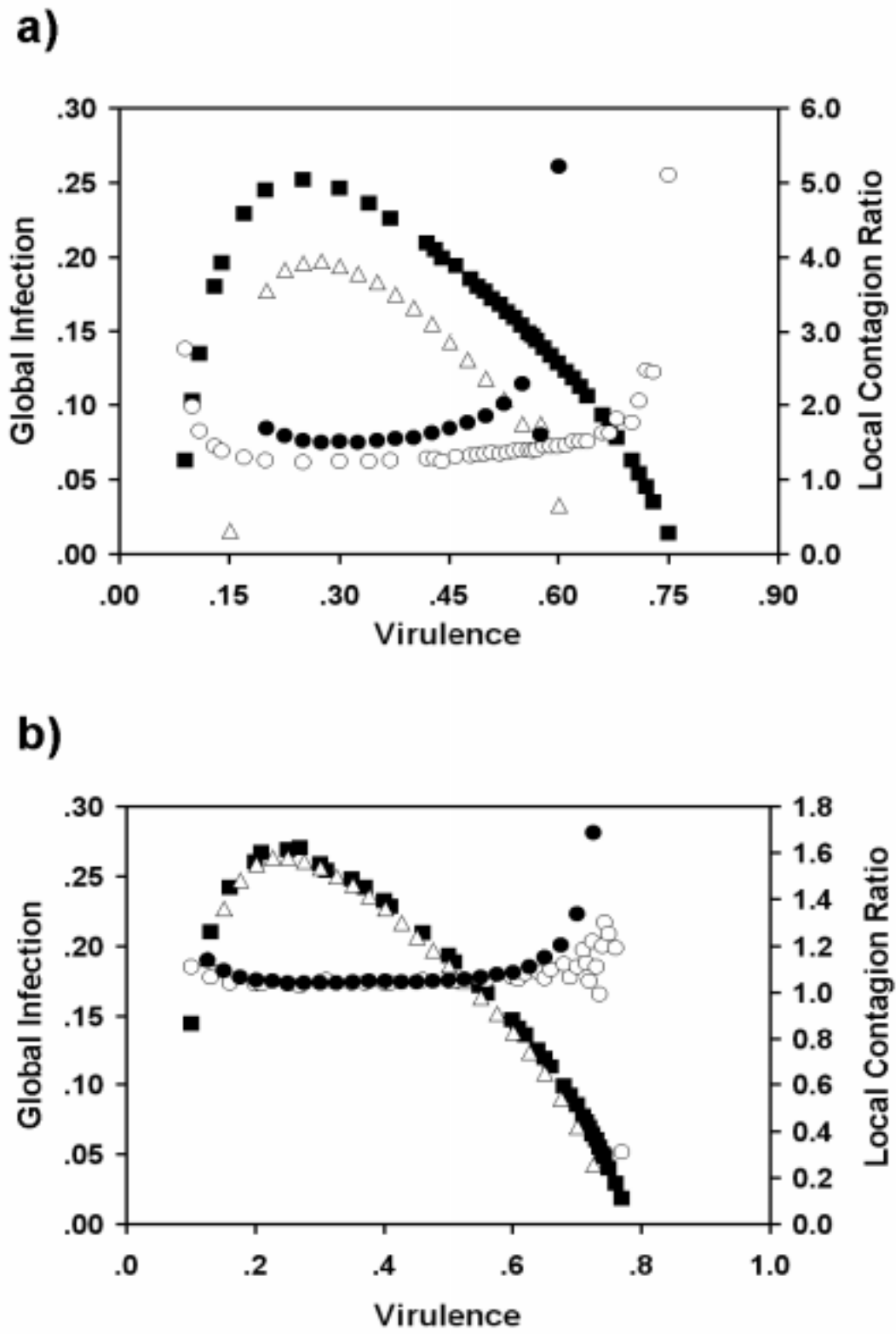


Table 1. Symbols used in spatially detailed model.

<u>Symbol</u>	<u>Meaning (Numerical value)</u>
R_0	Basic reproduction number of pathogen strain
J	Total number of lattice sites in spatial model
$s_k(t)$	Elementary state of site k at time t
σ_k	Interaction neighborhood around lattice site k
N	Neighborhood size ($N = 8, 48$)
B	Host reproductive-effort probability ($B = 1$)
b	Per-site probability host attempts propagation
β_A	Avirulent strain infection probability
β_V	Virulent strain infection probability
γ	Superinfection probability
$n(s)$	Number of sites on σ_k with state s
μ_S	Susceptible host's mortality probability (0.05)
μ_A	Mortality probability with avirulent infection
μ_V	Mortality probability with virulent infection
α	Shapes infection-transmission function
f	Weight equalizing total infectiousness for different transmission-virulence functions
ψ	Sets concavity/convexity of superinfection probability ($\psi = 0.2, 1.2$)

Table 2. Symbols introduced in mean-field model.

<u>Symbol</u>	<u>Meaning</u>
$\rho_0(t)$	Global density of open sites with state s , time t
$\rho_s(t)$	Global susceptible density
$\rho_A(t), \rho_V(t)$	Global density of avirulent, virulent infection
$\rho(t)$	Global density of hosts at time t
ε	Virulence mutation, resident-invader difference

Table 3. Symbols introduced in pair approximation.

<u>Symbol</u>	<u>Meaning</u>
$P[ij]$	Block probability, states i and j
$P_i[i]$	Global density, sites with state i
$\lambda(t)$	Probability site, state unknown, attempts to colonize open site
$\theta_A(t)$	Probability susceptible contacts avirulent infection at site with state unknown
$\theta_V(t)$	Probability susceptible contacts virulent infection at site with state unknown
$\theta_{si}(t)$	Probability avirulently infected host contacts virulent infection at site with state unknown